

Mining key circadian biomarkers for major depressive disorder by integrating bioinformatics and machine learning

Yuhe Shi¹, Jue Zhu¹, Chaowen Hou¹, Xiaoling Li¹, Qiaozhen Tong¹

¹Department of Pharmacy, Hunan University of Chinese Medicine, Changsha, Hunan 410208, China

Correspondence to: Qiaozhen Tong; **email:** qztong88@126.com, <https://orcid.org/0009-0003-6395-4872>

Keywords: major depressive disorder, circadian rhythm, bioinformatics, machine learning, biomarker, immune infiltration, drug prediction

Received: December 1, 2023

Accepted: May 3, 2024

Published: June 13, 2024

Copyright: © 2024 Shi et al. This is an open access article distributed under the terms of the [Creative Commons Attribution License](https://creativecommons.org/licenses/by/4.0/) (CC BY 4.0), which permits unrestricted use, distribution, and reproduction in any medium, provided the original author and source are credited.

ABSTRACT

Objective: This study aimed to identify key clock genes closely associated with major depressive disorder (MDD) using bioinformatics and machine learning approaches.

Methods: Gene expression data of 128 MDD patients and 64 healthy controls from blood samples were obtained. Differentially expressed genes were identified and weighted gene co-expression network analysis (WGCNA) was first performed to screen MDD-related key genes. These genes were then intersected with 1475 known circadian rhythm genes to identify circadian rhythm genes associated with MDD. Finally, multiple machine learning algorithms were applied for further selection, to determine the most critical 4 circadian rhythm biomarkers.

Results: Four key circadian rhythm genes (ABCC2, APP, HK2 and RORA) were identified that could effectively distinguish MDD samples from controls. These genes were significantly enriched in circadian pathways and showed strong correlations with immune cell infiltration. Drug target prediction suggested that small molecules like melatonin and escitalopram may target these circadian rhythm proteins.

Conclusion: This study revealed discovered 4 key circadian rhythm genes closely associated with MDD, which may serve as diagnostic biomarkers and therapeutic targets. The findings highlight the important roles of circadian disruptions in the pathogenesis of MDD, providing new insights for precision diagnosis and targeted treatment of MDD.

INTRODUCTION

Major depressive disorder (MDD) is a prevalent and debilitating psychiatric condition characterized by persistent low mood, diminished interest, sleep disturbances, feelings of worthlessness, and recurrent thoughts of death [1–2]. According to the latest cross-national data, more than half of the global population can expect to develop one or more mental disorders by the age of 75 years, with similar rates between males and females. These disorders typically first emerge during childhood, adolescence, or young adulthood, with a peak incidence around age 15 years and a median age of onset of 19–20 years [3]. As a

leading cause of disability worldwide, MDD imposes a substantial burden on individuals, families, and healthcare systems [4, 5]. Despite the availability of pharmacological and psychotherapeutic interventions, current treatments for MDD have significant limitations. Antidepressant medications, such as selective serotonin reuptake inhibitors and glutamate modulators, often have suboptimal efficacy, high relapse rates, and undesirable side effects [6, 7]. Cognitive-behavioral therapy, a common psychological intervention, also faces challenges in terms of patient accessibility and long-term effectiveness. Importantly, the underlying pathogenesis of MDD remains incompletely understood,

hindering the development of more effective and personalized treatment strategies.

The multifactorial nature of MDD involves complex interactions between genetic, neurobiological, and environmental factors. Disturbances in neurotransmitters systems, signaling pathways, the hypothalamic-pituitary-adrenal (HPA) axis, and inflammatory responses have all been implicated in the pathogenesis of MDD [8]. Moreover, altered expression of biomarkers, such as brain-derived neurotrophic factor (BDNF), has been closely linked to the onset and progression of disorder [9]. Elucidating the clinical molecular characteristics of MDD is crucial for improving our understanding of its pathogenesis and enabling the development of novel diagnostic and therapeutic approaches.

Emerging evidence suggests that disruptions in circadian rhythms, the endogenous 24-hour cycles that regulate physiological processes, may play a pivotal role in the pathophysiology of MDD [10–12]. Patients with MDD commonly exhibit circadian rhythm disturbances, such as sleep abnormalities, disrupted temperature rhythms, endocrine dysregulation, and metabolic abnormalities [13]. These observations indicate that the biological clock governing circadian rhythms in MDD patients may be dysfunctional. Notably, some circadian genes, such as Brain and Muscle ARNT-Like 1 (BMAL1), have been demonstrated to significantly influence the onset and progression of MDD [14]. However, the specific roles of circadian mechanisms in MDD remain underexplored, and many potentially important circadian genes associated with the disorder are yet to be identified.

Importantly, this study adopts an integrative approach by combining advanced bioinformatics analysis and machine learning algorithms to systematically investigate the role of circadian rhythm disturbances in MDD [15]. Unlike previous studies that have primarily focused on individual circadian genes, our comprehensive analysis aims to identify novel key circadian biomarkers that can distinguish MDD patients from healthy controls. Moreover, we further explore the functional relevance of these circadian biomarkers in MDD pathogenesis, such as their associations with immune cell infiltration, and utilize computational drug discovery methods to predict potential therapeutic compounds targeting the key circadian proteins. The findings from this multilayered investigation are expected to provide new mechanistic insights into the circadian rhythm-MDD connection and pave the way for developing more effective diagnostic and treatment strategies for this debilitating psychiatric disorder.

MATERIALS AND METHODS

Data collection

Two gene expression profiles (GSE98793 and GSE76826) related to MDD were retrieved from the Gene Expression Omnibus database (GEO, <https://www.ncbi.nlm.nih.gov/geo/>). GSE98793 and GSE76826 were from GPL570 and GPL17077 platforms, respectively. The GSE98793 dataset included 128 patients with MDD and 64 healthy controls. The GSE76826 dataset included 12 patients with MDD and 12 healthy controls. MDD was determined by SIGH-D scores higher than 8. Gene expression in both datasets was from human blood samples.

In addition, a total of 1475 human circadian rhythm genes (CRGs) were obtained from the Circadian Gene Database (CGDB, <http://cgdb.biocuckoo.org/>), MSigDB database (<https://www.gsea-msigdb.org/gsea/msigdb/>) and Genecards database (<https://www.genecards.org/>) (Supplementary Table 1). These genes were used as the basis of this study.

In this study, GSE98793 was used as the training set for screening potential therapeutic targets for MDD and selecting circadian rhythm related key genes. The GSE76826 dataset was used as the validation set to verify the reliability of the prediction model.

Identification of circadian rhythm genes (CRGs) related to MDD

Differential expression analysis

The GSE98793 dataset was used for differential gene expression analysis. First, the gene chip data in GSE98793 were normalized using the limma package in R software, and the genes were annotated. Differentially expressed genes (DEGs) between MDD patients and normal samples in the training set were screened with a threshold of P -value < 0.05 .

Weighted gene co-expression network (WGCNA) analysis

We further analyzed the differential genes in MDD using WGCN analysis. Through WGCNA, functionally related gene co-expression modules were identified, and an unsigned co-expression network was constructed. First, clustering analysis of differential gene expression profiles was performed, and outliers were removed. Next, a “soft” threshold (β) value generated by the “pickSoftThreshold” algorithm was selected to construct an adjacency matrix and convert it to a topological overlap matrix (TOM). Then, high co-expression gene modules were generated by dynamic tree cutting.

Finally, gene significance (GS) and module membership (MM) were calculated to determine the correlation between module feature genes (ME) and clinical traits. Differentially expressed genes that were closely related to the pathogenesis of MDD were screened in modules with GS >0.5, MM >0.5, and *P*-value < 0.05.

Identification of CRGs related to MDD

By intersecting the differential co-expressed genes obtained from the WGCNA network with the 1475 CRGs downloaded from the database, common genes were determined. These common genes were CRGs that influence the occurrence and development of MDD.

Construction of protein-protein interaction (PPI) networks and functional enrichment analysis of CRGs

Protein-protein interaction (PPI) network analysis was performed for the CRGs related to MDD using the STRING online server (<https://string-db.org/>). Cytoscape 3.7.2 was used to visualize the results, and the degree parameters of the nodes in the network were analyzed.

To investigate the potential biological functions and signaling pathways of CRGs in the pathogenesis of MDD, functional enrichment analysis of MDD-related CRGs was performed using the online DAVID database (<https://david.ncifcrf.gov/>). Gene Ontology (GO) functional annotation and Kyoto Encyclopedia of Genes and Genomes (KEGG) functional enrichment analyses were applied for the analysis of MDD-related CRGs. The GO analysis covered three dimensions: biological processes (BP), cellular components (CC), and molecular functions (MF). It is a systematic method and process for annotating genes and their expression products. KEGG is an integrated database of genomic, chemical and systemic functional information, which is widely used for enrichment annotation of gene pathways. GO and KEGG analyses used a screening criterion of *P*-value < 0.05, and results were visualized.

Identification of key CRGs related to MDD using machine learning

Three machine learning algorithms including least absolute shrinkage and selection operator (LASSO) logistic regression, support vector machine-recursive feature elimination (SVM-RFE), and random forest (RF) were utilized to identify key feature molecules among the differentially expressed CRGs in the GSE98793 database.

Key CRGs were selected based on LASSO model, SVM-RFE algorithm, and random forest model using R packages “rms”, “e1071”, and “randomForest”, respectively. Finally, the overlapping genes identified by the three machine learning algorithms were determined as key diagnostic circadian rhythm biomarkers with critical roles in predicting MDD.

Validation of expression and ROC analysis for key CRGs

The expression levels of key CRGs in blood samples from MDD patients and normal controls were measured and verified by Wilcoxon rank sum test using the two datasets. First, the expression levels of key CRGs were determined in MDD patients and normal controls using the GSE98793 dataset as the training set. Then, the expression of these key CRGs was validated in the GSE76826 dataset.

To further test the accuracy of the key CRG selection in this study, and evaluate the diagnostic value of key CRGs as MDD biomarkers, receiver operating characteristic (ROC) curve analysis was performed on the GSE98793 and GSE76826 datasets using the “pROC” package in R.

Immune infiltration analysis

CIBERSORTx (<https://cibersortx.stanford.edu/>), a computational tool based on single-cell RNA sequencing (scRNA-seq) data, can be utilized to infer the composition and relative proportion of immune cells in bulk tissues [16]. To further elucidate the relationship between MDD and immune cells, we uploaded the gene matrix data containing blood samples from depressed patients and normal controls to the CIBERSORTx database, and calculated the correlations between these genes and 22 types of immune cells. Wilcoxon rank sum test was used for analysis, and *p* < 0.05 was considered statistically significant. Subsequently, we also examined the distribution of potential key CRGs in immune cells as well as changes occurring in blood samples from normal controls versus depressed patients.

Prediction of potential small molecule drugs

To uncover potential small molecule drugs that regulate key CRGs, we utilized Drug-Gene Interaction Database (DGIdb 4.0, <http://dgidb.genome.wustl.edu/>) and Connectivity Map (CMap) database (<https://clue.io>) simultaneously. DGIdb integrates drug-gene, drug-variant, and drug-tumor interactions from various public databases, enabling rapid discovery of potential drug targets and mechanisms of action [17]. CMap is a reliable, well-recognized genomics-based tool for

discovering drugs to prevent diseases, which can predict drugs that may reverse or induce the expression of genes encoding a biological state through enrichment scores of positive and negative values [18]. We preferentially selected DGIdb results with higher-ranking scores and CMap database results with negative enrichment scores.

Molecular docking validation

To validate the direct targeting interactions between key CRGs and predicted drugs, molecular docking was performed using Discovery Studio software (version 2019). First, three-dimensional structure files of key circadian rhythm target proteins and drugs were downloaded from the RCSB Protein Data Bank (PDB, <http://www.rcsb.org/>) and PubChem (<https://pubchem.ncbi.nlm.nih.gov/>) databases, respectively. Then, these protein and small molecule structures were imported into Discovery Studio software. To prepare for docking calculations, proteins and small molecules were preprocessed, including cleaning small molecule structures, adding partial charges, predicting small molecule protonation states to make them suitable for docking. Next, we defined the binding pocket regions of interest on the three-dimensional structures of the target proteins as the docking sites. Finally, LibDock in Discovery Studio was utilized for automatic molecular docking, which searches for the optimal binding modes between ligands and target proteins by rigid docking and inverse docking algorithms within the defined docking sites. After docking, LibDock scores were calculated for each ligand-target protein complex. Higher LibDock scores indicate stronger binding affinity between the ligand and target protein. Through this molecular docking process, we can evaluate the binding affinities between small molecule drugs candidates and the target proteins, thereby guiding drug optimization of drug design.

Availability of data and materials

The datasets analyzed during the current study are available in the Gene Expression Omnibus repository (Accession Number: GSE98793 and GSE76826).

RESULTS

Identification of DEGs and WGCNA analysis

To explore genes associated with the occurrence and development of MDD, we first performed differential expression analysis on 64 normal samples and 128 MDD serum samples in GSE98793 dataset. The results showed that 1458 DEGs were identified between MDD patients and normal samples, including 676 down-

regulated and 782 up-regulated genes (Figure 1A). The hierarchical clustering of DEGs was shown in Figure 1B. No abnormal samples were detected after clustering analysis with high threshold β of 12 (Figure 1C). Based on the dynamic tree cut algorithm, 8 gene modules were constructed with a minimum module size of 28, deep split of 4, and a maximum module distance of 0.25, including turquoise, brown, blue, pink, yellow, black, green and grey module (Figure 1D). Upon analyzing the connectivity of the module eigengenes (MEs), it was discovered that when the separation among modules exceeded 0.25, the genes within each module could operate independently (Figure 1E). By calculating the correlation coefficients between the modules and the clinical features of Major Depressive Disorder (MDD), it was found that all modules were significantly associated with MDD (Figure 1F). According to the criteria of $|MM|>0.5$ and $|GS|>0.5$, 954 genes highly correlated with MDD were identified from the 8 co-expressed gene modules (Figure 2). These hub genes exhibited expression patterns closely related to MDD phenotype, and were therefore defined as MDD-related targets.

Screening of MDD-related CRGs

Given the well-established relationship between circadian rhythm dysregulation and MDD, we sought to identify the key circadian genes associated with MDD pathogenesis. By intersecting the 954 MDD-related targets identified in the previous step with a comprehensive list of 1475 known CRGs, we successfully identified 75 common targets between the two gene sets (Figure 3). These 75 overlapping genes were considered as the MDD-related CRGs, which may play crucial roles in the circadian rhythm disruptions underlying MDD development and progression.

PPI network construction and functional enrichment analysis

To gain deeper insights into the molecular mechanisms underlying the involvement of the 75 identified MDD-related CRGs, we constructed a protein-protein interaction (PPI) network using these genes (Figure 4A). The complex interconnections observed within this PPI network suggest that these CRGs may function in a coordinated manner to influence MDD pathogenesis.

To further elucidate the biological functions and pathways associated with these 75 MDD-related CRGs, we performed GO and KEGG enrichment analyses (Figure 4B–4D). The top 10 enriched GO terms covered a wide range of biological process, cellular component and molecular function. In biological process category, these CRGs were significantly enriched in transcription

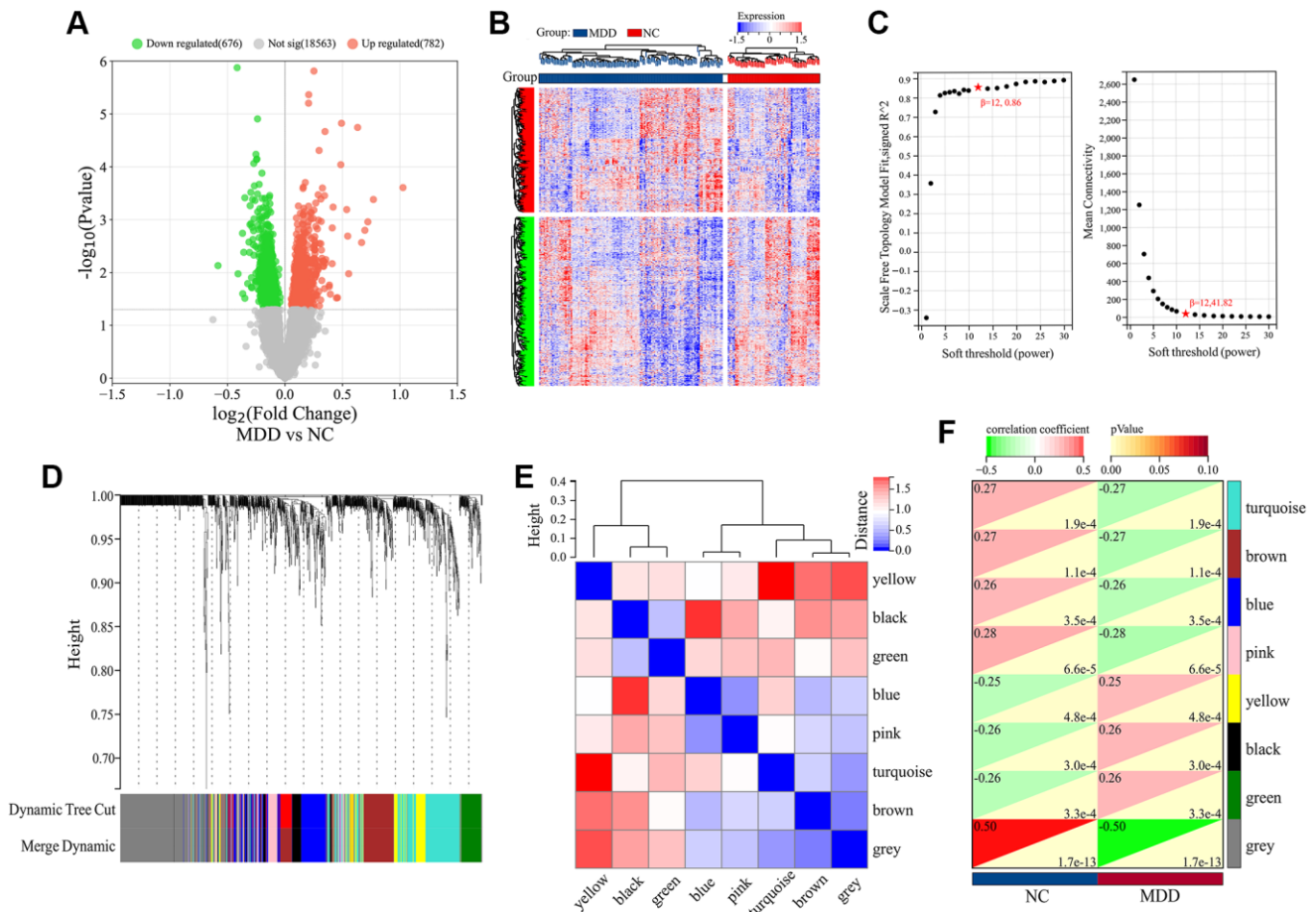


Figure 1. Differential expression and WGCNA analysis of DEGs in GSE98793 dataset. (A) Volcano plot of DEGs. (B) Hierarchical clustering of DEGs. (C) Scale independence and Mean connectivity as a function of soft-thresholding powers. (D) Cluster dendrogram. (E) Heatmap based on gene connectivity of modules. (F) Heatmap of clinical-trait associations.

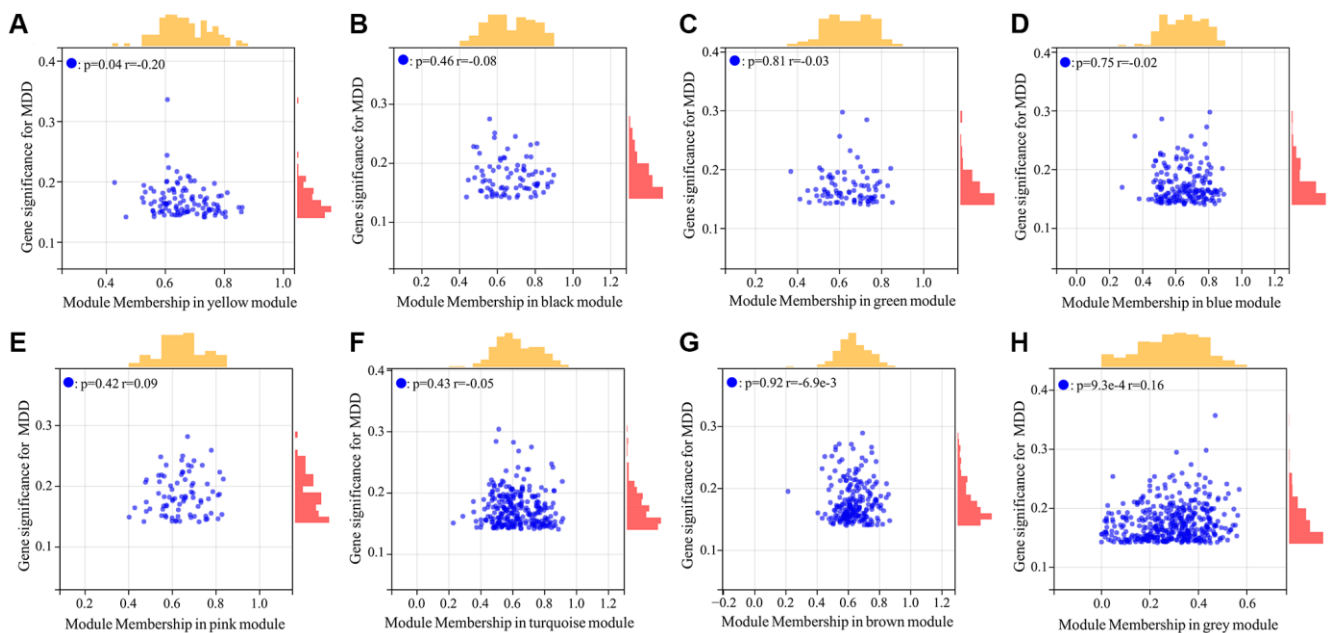


Figure 2. Scatter plot analysis of hub genes highly associated with MDD from 8 co-expressed gene modules. (A-H) Represented yellow, black, green, blue, pink, turquoise, brown, grey module respectively.

regulation, telomerase activity control, response to hypoxia, circadian regulation, and tau-protein kinase activity modulation. The cellular component analysis

revealed the localization of these CRGs in neuromuscular junction, melanosome, cell surface and extracellular exosome. Regarding molecular function,

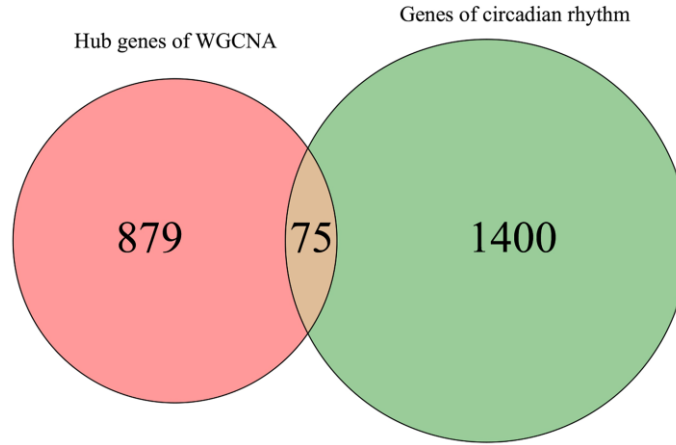


Figure 3. Venn diagram for screening MDD-related CRGs.

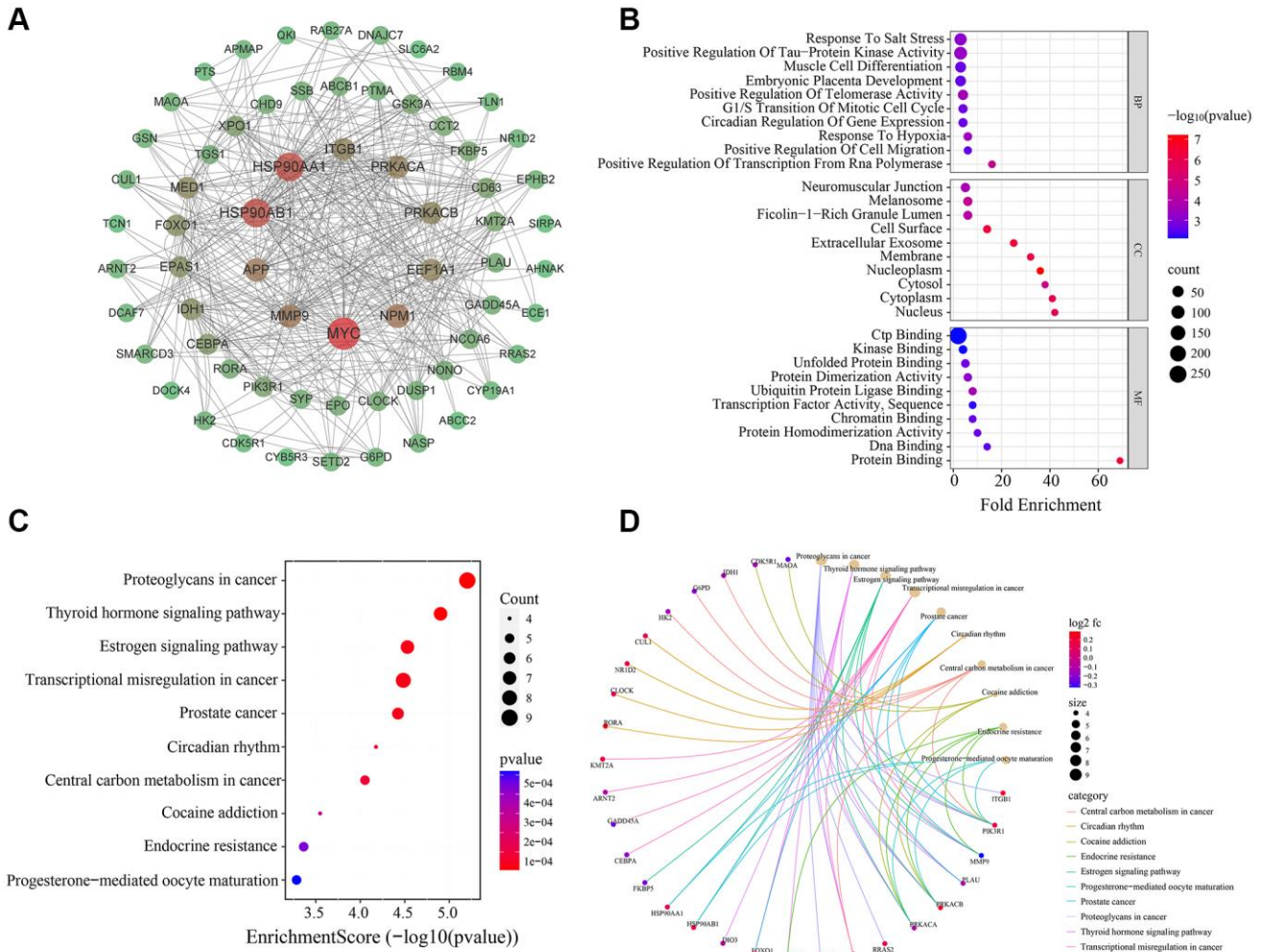


Figure 4. Bioinformatics analysis of 75 MDD-related CRGs. (A) PPI network of 75 MDD-related CRGs. Nodes represent targets and edges represent interactions. (B) Bubble chart of GO enrichment results. (C) Bubble chart of KEGG pathway enrichment results. (D) Enrichment plot of targets in pathways.

the CRGs were found to be involved in CTP binding, kinase binding, unfolded protein binding, and protein activity.

The KEGG pathway analysis identified the top 10 significantly enriched pathways, including proteoglycans in cancer, thyroid hormone signaling pathway, estrogen signaling pathway, transcriptional misregulation in cancer, circadian rhythm, cocaine addiction, and endocrine resistance. These results suggest that the MDD-related CRGs identified in this study may play crucial roles in regulating diverse biological processes and signaling pathways, particularly those involved in circadian rhythm, neuroendocrine function, and cancer-related pathways, which are closely linked to MDD pathogenesis.

Screening of key MDD-related CRGs using machine learning

To further identify the key CRGs most closely associated with MDD, we applied three machine learning methods - LASSO regression, SVM-RFE, and Random Forest - to the 75 MDD-related CRGs identified previously. First, we constructed a LASSO regression model to predict MDD status using the 75 CRGs. Ten-fold cross validation determined the optimal regularization parameter λ as 0.03 (Figure 5A). The LASSO model identified 21 feature genes that could accurately distinguish MDD samples from normal controls (Figure 5B). Next, we employed the Random Forest algorithm to rank the 75 CRGs by feature importance. The top 30 genes were selected as key feature genes (Figure 5C, 5D). We also performed SVM-RFE analysis, which identified 22 genes with good classification accuracy between MDD and normal samples (Figure 5E, 5F). These 22 genes were ranked by Avg rank (Figure 5G). By integrating the results of three machine learning algorithms, we finally identified 4 common key CRGs: ABCC1 (ATP-binding cassette subfamily C member 2), APP (Amyloid precursor protein), HK2 (Hexokinase 2), and RORA (RAR related orphan receptor A) (Figure 5H). These 4 key CRGs were considered the most promising potential biomarkers of circadian rhythm dysfunction in MDD patients.

Expression analysis and dataset validation of key CRGs

To validate the clinical relevance of the 4 key CRGs (ABCC2, APP, HK2, and RORA) identified in the previous section, we examined their expression in blood samples from MDD patients and healthy controls using the GSE98793 dataset as a training set and GSE76826 as an independent validation set. As illustrated in

Figure 6A, 6C, three key CRGs - ABCC2, APP, and HK2 - exhibited significantly up-regulated in the blood samples of MDD patients relative to healthy controls, across both the training and validation datasets. In contrast, the expression of the circadian rhythm gene RORA was significantly down-regulated in MDD samples. To further evaluate the diagnostic potential of these 4 key CRGs as biomarkers for MDD-related circadian rhythm dysfunction, we performed receiver operating characteristic (ROC) curve analysis. As illustrated in Figure 6B, 6D, the area under the ROC curve (AUC) values for all 4 key CRGs were greater than 0.70 in both the training and validation datasets, suggesting they have good diagnostic accuracy in distinguishing MDD patients from healthy individuals.

Analysis of immune cell infiltration

To explore the potential involvement of immune dysregulation in MDD, we first compared the abundance of 22 different immune cell types between blood samples from MDD patients and healthy controls. As shown in Figure 7A, the immune cell composition profiles were distinct between the two groups. Correlation analysis of immune cell populations revealed several notable relationships (Figure 7B). Neutrophils were strongly negatively correlated with Monocytes ($r = -0.74$) and T cells CD8 ($r = -0.71$), while Macrophages M1 was positively correlated with T cells CD4 memory activated ($r = 0.59$). Further comparison of the immune cell infiltration levels between MDD and normal blood samples identified several significantly altered cell types (Figure 7C). Neutrophils were significantly increased, while B cells memory, T cells CD8, Dendritic cells resting were significantly decreased in the blood of MDD patients compared to healthy controls.

To investigate the potential links between the 4 key CRGs (ABCC2, APP, HK2, and RORA) and immune cell infiltration, we performed correlation analyses (Figure 8A–8D). ABCC2 was significantly positively correlated with Neutrophils and activated NK cells, but negatively correlated with T cells CD8 and Monocytes. APP showed positively correlated with Monocytes and resting NK cells, but negatively correlated with resting Dendritic cells and B cells memory. HK2 was positively associated with Neutrophils and activated NK cells, while negatively associated with T cells CD8 and B cells memory. Interestingly, RORA exhibited positive correlations with T cells CD8 and Monocytes, but negative correlations with Neutrophils and naive T cells CD4. These results suggest that the key CRGs identified in this study may be closely linked to the dysregulation of specific immune cell populations in MDD, which could contribute to the pathogenesis of the disease.

Further investigation into the underlying mechanisms is warranted.

Prediction of small molecule drugs and molecular docking

To identify potential small molecule drugs that could modulate the imbalanced circadian rhythms associated

with the 4 key CRGs (APP, RORA, ABCC2, and HK2), we queried the DGIdb and CMap databases. For APP, the top 3 related compounds from the DGIdb database were Ferulic acid, Isochlorogenic acid B, Scyllitol. For RORA, only 2 corresponding compounds were found-Melatonin and Citalopram. The DGIdb search for ABCC2 yielded 4 top-ranked compounds: Talinolol, Tenofovir, Sulfinpyrazone, Cefamandole. Additionally,

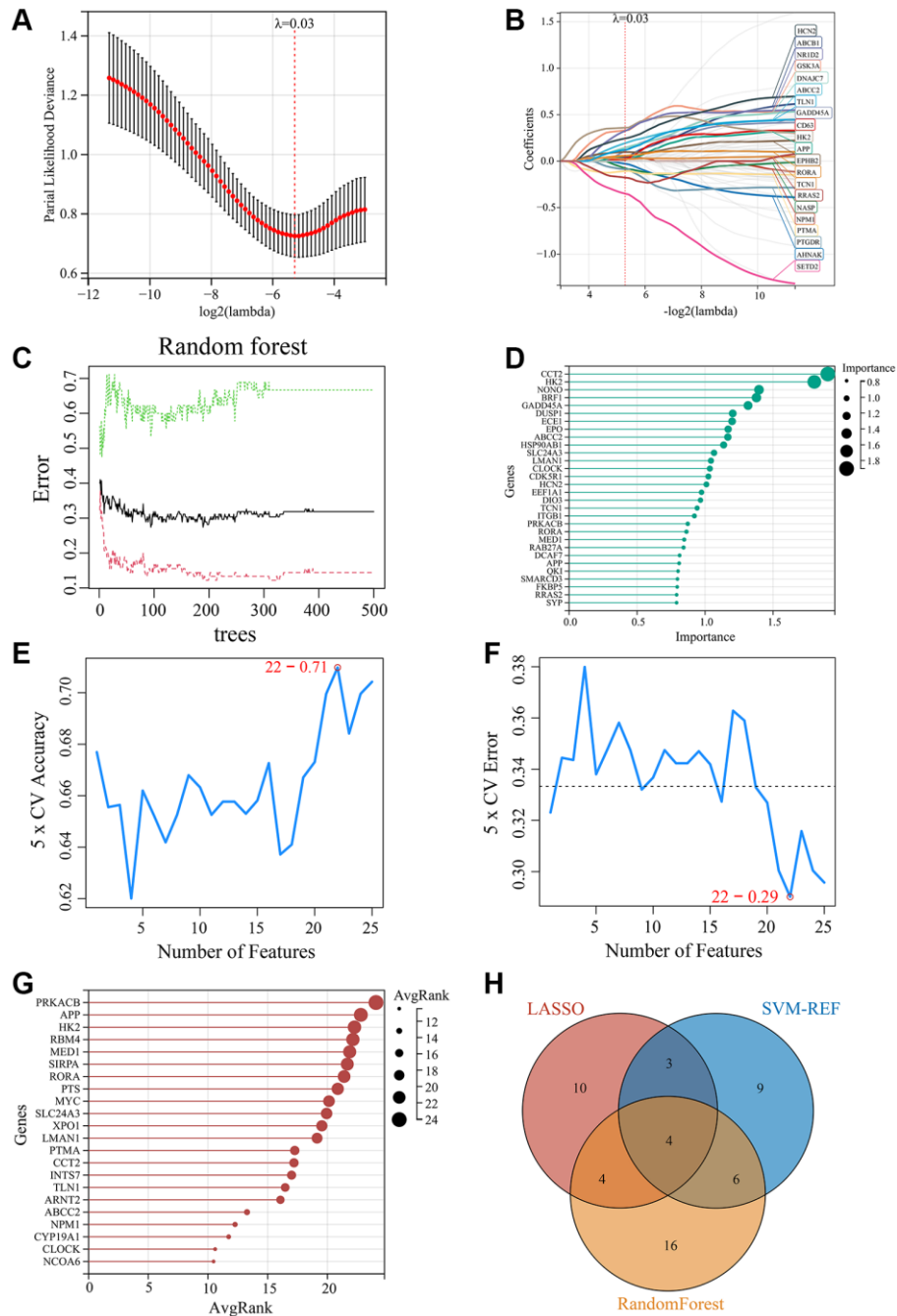


Figure 5. Screening of key MDD-related CRGs using machine learning methods. (A) Optimal λ selection for LASSO regression model. (B) LASSO coefficient profiles of the 21 feature genes. (C) Top 30 feature importance from random forest algorithm. (D) Top 30 important genes ranked by random forest algorithm. (E) Accuracy rate plot of SVM-RFE model. (F) Error rate plot of SVM-RFE model. (G) Top 22 genes with lowest error rate ranked by SVM-RFE. (H) Venn diagram for screening of the 4 key CRGs (ABCC1, APP, HK2, and RORA) by integrating LASSO, SVM-RFE and Random Forest algorithms.

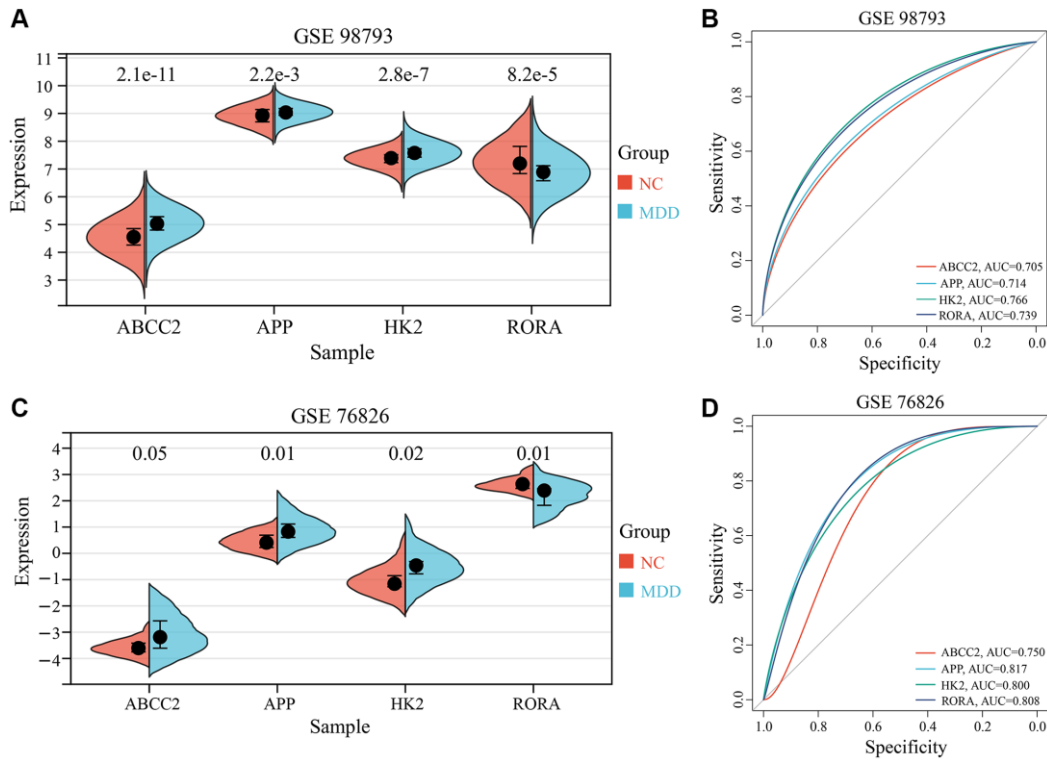


Figure 6. Expression analysis and ROC curves of 4 key CRGs. (A, B) Box plots and ROC curves of 4 key CRGs from training set (GSE98793). (C, D) Box plots and ROC curves of 4 key CRGs from validation set (GSE76826).

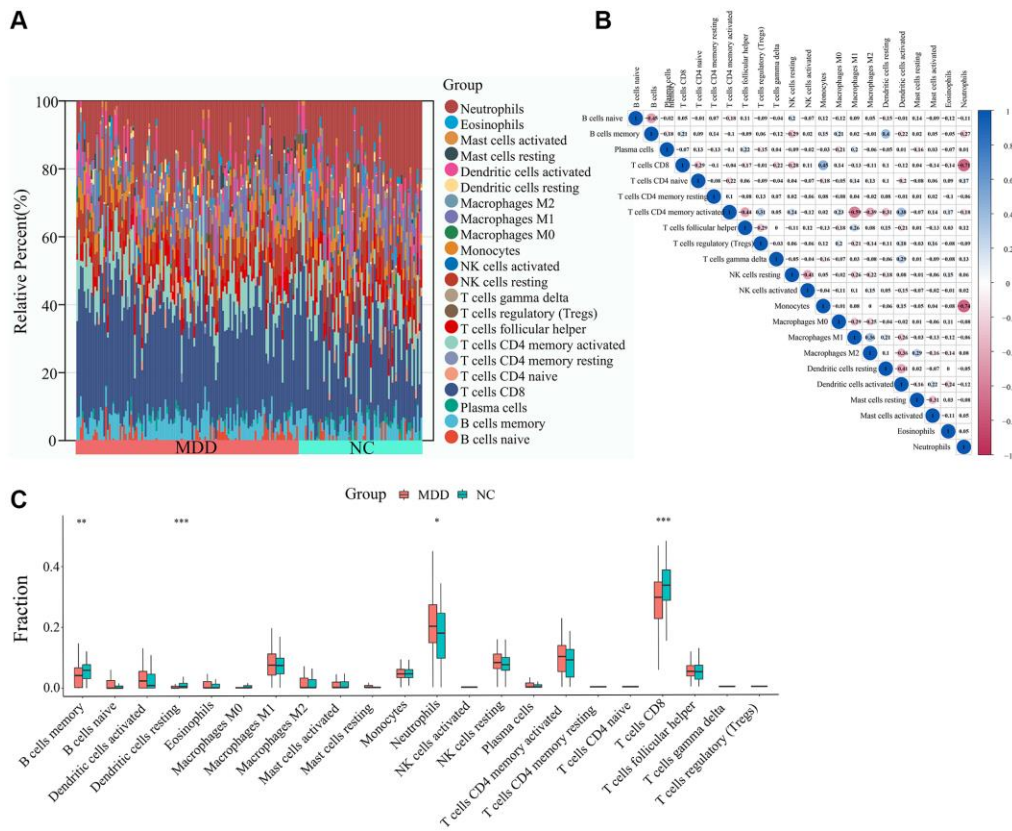


Figure 7. Immune cell infiltration analysis. (A) Abundance of immune cells in each sample. (B) Correlation analysis between immune cells. (C) Differential analysis of immune cell infiltration levels between MDD and normal blood samples.

3-Bromopyruvic acid was the sole compound associated with HK2 in the CMAP database (Figure 9).

To further validate the potential interactions between these small molecule drugs and the 4 key CRGs, we performed molecular docking analysis. As shown in Table 1, APP, RORA, ABCC2 exhibited good docking interactions with their respective predicted compounds. Specifically, Isochlorogenic acid B had the tightest binding with APP (LibDock score of 126.536), Melatonin showed the highest docking value with RORA (125.850), and Cefamandole exhibited the highest affinity to ABCC2 (110.523). In contrast, 3-Bromopyruvic acid had a relatively low LibDock score of 53.369 with HK2, suggesting the need for further experimental verification of its interaction. The top 4 docking results are presented in Figure 10. These findings provide strong bioinformatics support

for the potential of small molecule drugs to modulate the key circadian rhythm genes associated with MDD pathogenesis. Further in vitro and in vivo studies are warranted to validate the therapeutic implications of these drug-target interactions.

DISCUSSION

MDD is a debilitating mental illness with high mortality and disability. Recent epidemiological surveys reveal that the number of individuals suffering from MDD worldwide surpasses 350 million, with the COVID-19 pandemic markedly exacerbating the global burden of depression [19]. Emerging evidence has highlighted the significance of circadian rhythm abnormalities in the pathogenesis of MDD. Disruptions in sleep disorders patterns, diurna activity, hormone secretion, and other physiological processes regulated by the circadian clock

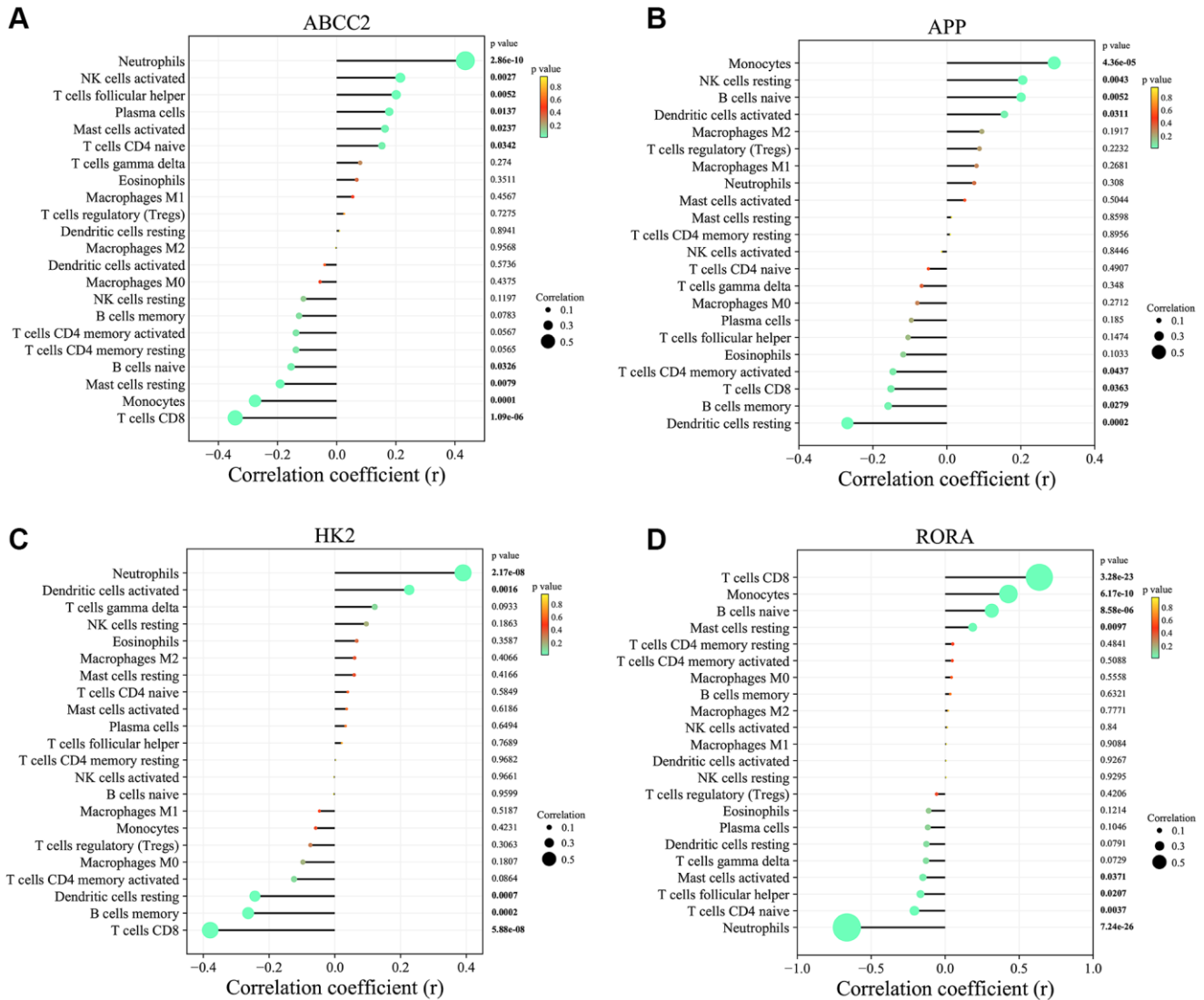


Figure 8. Correlation analysis between key circadian rhythm genes and immune cell infiltration levels. (A) ABCC2. (B) APP. (C) HK2. (D) RORA.

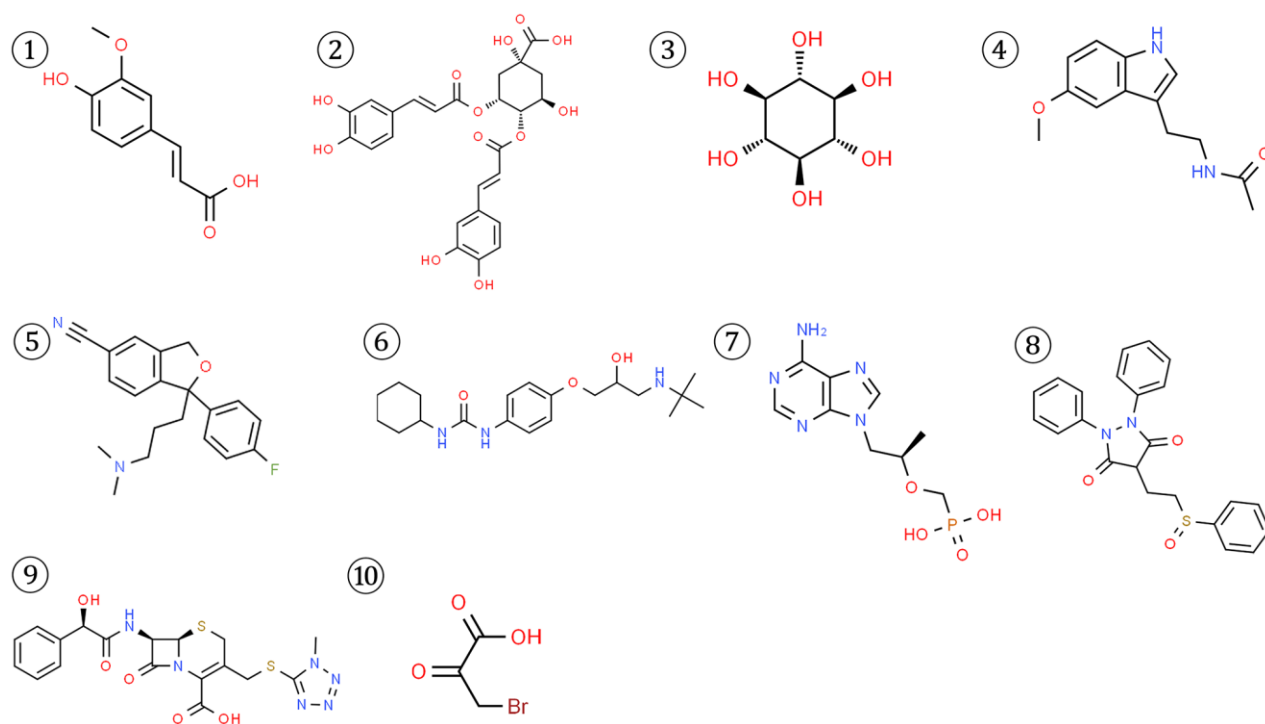
Table 1. Molecular docking results between 4 key CRGs and predicted drugs.

Number	Name	Database	Target	Molecular formula	Interaction score	Libscore
1	Ferulic acid	DGIdb	APP	C ₁₀ H ₁₀ O ₄	3.99	105.341
2	Isochlorogenic acid B	DGIdb	APP	C ₂₅ H ₂₄ O ₁₂	3.99	126.536
3	Scyllitol	DGIdb	APP	C ₆ H ₁₂ O ₆	3.99	67.178
4	Melatonin	DGIdb	RORA	C ₁₃ H ₁₆ N ₂ O ₂	2.38	125.850
5	Citalopram	DGIdb	RORA	C ₂₀ H ₂₁ FN ₂ O	1.25	111.481
6	Talinolol	DGIdb	ABCC2	C ₂₀ H ₃₃ N ₃ O ₃	1.17	110.625
7	Tenofovir	DGIdb	ABCC2	C ₉ H ₁₄ N ₅ O ₄ P	0.97	110.189
8	Sulfinpyrazone	DGIdb	ABCC2	C ₂₃ H ₂₀ N ₂ O ₃ S	0.78	97.771
9	Cefamandole	DGIdb	ABCC2	C ₁₈ H ₁₈ N ₆ O ₅ S ₂	0.78	110.523
10	3-Bromopyruvic acid	cMAP	HK2	C ₃ H ₃ BrO ₃	-0.4368	53.369

represent core features of depressive disorders [11, 20–21]. While some CRGs located in the suprachiasmatic nucleus region of the hypothalamus, such as 5-hydroxytryptamine (5-HT), Basic helix-loop-helix ARNT-like protein 1 (BMAL1), Peroxidase 1-3 (Per 1-3), Nuclear receptor subfamily 1 group D member 1 (NR1D1), and D site-binding protein (DBP), have been observed in patients with MDD, the intricate functions of these CRGs pose formidable obstacles to their utilization as potential targets for the prevention, diagnosis, and treatment of the disorder [22, 23]. Fortunately, the advent of bioinformatics and machine

learning techniques has rendered the elucidation of disease pathogenic mechanisms and the identification of prospective disease biomarkers more feasible endeavors.

In the present study, we endeavored to synergistically leverage transcriptomic, bioinformatic, and machine learning approaches to explore potential CRGs biomarkers and investigate the influence of CRGs on the pathogenesis of MDD. Firstly, our findings revealed that several commonly disease-associated targets, such as RORA, Nuclear receptor subfamily 1 group D

**Figure 9. Structures of 10 potential small molecule drugs predicted to be associated with the 4 key CRGs from DGIdb and CMap databases.**

member 2 (NR1D2), Circadian locomotor output cycles protein kaput (CLOCK), and Cullin-1 (CUL1), were significantly enriched among CRGs within the circadian rhythm pathway. RORA can activate the expression of NR1D2, while NR1D2 in turn inhibits RORA, showing reciprocal regulation between them. Additionally, both RORA and NR1D2 can activate the transcription of circadian genes CLOCK, BMAL1, Cryptochrome-1

(CRY1) via ROM elements [24, 25]. As a transcriptional activator, CLOCK can activate the expression of downstream genes such as Per and Cry through the E-box (Enhancer element) element [26]. The CLOCK-BMAL1 complex can also activate the transcription of CUL1, promoting the degradation of circadian proteins [27]. The evidence presented above indicates that circadian rhythm disruption represents a

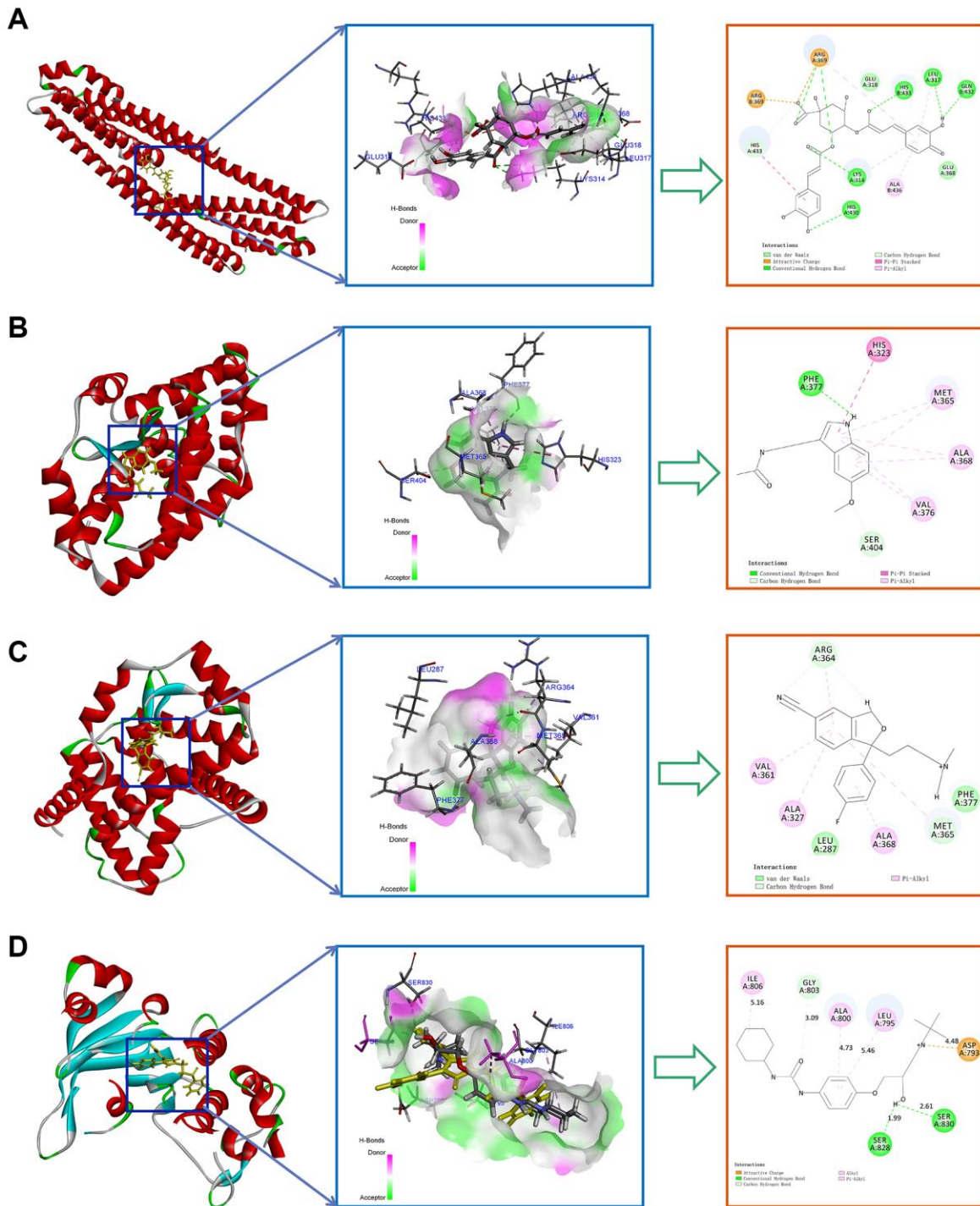


Figure 10. Top molecular docking results for 4 key CRGs and potential drugs. (A) Isochlorogenic acid B with APP. (B) Melatonin with RORA. (C) Citalopram with RORA. (D) Talinolol with ABCC2.

crucial factor influencing the pathogenesis of depressive disorders. It is noteworthy that we found the circadian mechanisms in MDD might also be associated with cancer-related pathways and hormone-related pathways. MDD is a comorbidity of various cancers that significantly increases the risk of other unhealthy outcomes in patients [28]. One study has shown that prostate cancer patients are prone to develop depressive mood after surgery due to disrupted circadian rhythms [29]. Alterations in hormone and endocrine functions play an important role in the pathophysiological mechanisms of MDD. Currently, preliminary trials of hormone therapy have shown good preliminary results in MDD, including corticotropin releasing factor antagonists, glucocorticoid receptor antagonists, thyroid hormone-based HPT axis treatments, and estrogen replacement therapy of HPG axis [30].

To further identify potential circadian biomarkers associated with MDD, we employed three machine learning techniques to improve the efficiency and accuracy of biomarker screening. A panel of 4 key CRGs—ABCC2, APP, HK2, and RORA—were identified and validated that are strongly associated with MDD. ABCC2, APP and HK2 were significantly upregulated, while RORA was downregulated in blood of MDD patients. The consistent differential expression patterns and robust diagnostic performance of these CRGs across two independent blood transcriptomic datasets provide compelling evidence for their potential utility as biomarkers of MDD-related circadian rhythm disturbances. ABCC2, also known as multidrug resistance-associated protein 2 (MRP2), belongs to the ATP-binding cassette (ABC) transporter family, participating in the transport of drugs and pathogenic metabolites [31]. It has been found that the expression and function of ABCC2 exhibit circadian rhythmic patterns, the transcription of which is inhibited by Rev-erba, a downstream gene of BMAL1/CLOCK [32]. Existing studies have demonstrated that the function of ABCC2 impacts the pharmacokinetics and pharmacodynamics of antidepressant medications, thereby influencing therapeutic outcomes [33]. ABCC2 may be implicated in the pathogenesis of MDD through its involvement in the transport of neurotransmitters and hormones across the blood-brain barrier. For instance, elevated plasma levels of 5-HT, a crucial antidepressant neurotransmitter, have been demonstrated to suppress ABCC2 expression [34]. This finding corroborates the trend observed in our research results. Moreover, ABCC2 also regulates the transport of glucocorticoids, which are critical mediators of the stress response and intimately associated with the onset and progression of depressive disorders [35]. APP is a transmembrane protein mainly located in synaptic regions of neurons, involved in regulating synapse formation, neurotropy

and neuroplasticity. The participation of APP in circadian mechanisms is associated with disruption of CLOCK/BMAL1 regulatory elements, interference with circadian gene expression, and disturbance of circadian rhythms [36, 37]. It is well-established that aberrant splicing and metabolism of the APP, leading to the production of beta-amyloid, constitutes the critical pathological basis for Alzheimer's disease. An accumulating body of evidence suggests the existence of a shared genetic foundation between MDD and Alzheimer's disease [38, 39]. These findings illustrate that APP also plays a pivotal role in the pathogenic mechanisms underlying depressive disorders. On one hand, aberrant APP metabolism and amyloid aggregation can induce neuronal injury and apoptosis, which is consistent with the hippocampal and cortical atrophy observed in patients with MDD [40]. On the other hand, APP also influences the expression of proteins associated with neuroplasticity, such as brain-derived neurotrophic factor (BDNF) and Postsynaptic density protein 95 (PSD-95), thereby disrupting synaptic remodeling, which may represent a critical molecular event in the onset of depressive episodes [41]. HK2 is a rate-limiting enzyme that catalyzes the phosphorylation of glucose and plays a key role in glycolysis. The involvement of HK2 in circadian mechanisms is associated with effects on glucose metabolism in the body. Singh Gurjit et al. found that HK2 in the brain of North American wood frogs exhibited circadian rhythmic expression changes, which was related to the regulation by the bHLH family transcription factor MondoA-MLX complex [42]. This study provided clues on the rhythm of biological clock and metabolism. Another study showed that specific deletion of the circadian gene BMAL1 would affect mRNA expression and activities of HK2 and phosphofructokinase 1 (PFK1) in tissues, further influencing systemic glucose homeostasis [43]. The above studies demonstrated the key evidence of HK2 in circadian rhythms and glucose metabolism in the body. The RORA gene encodes the retinoic acid-related orphan receptor alpha (ROR α), a member of the nuclear receptor superfamily. ROR α plays a crucial role in regulating various physiological processes, including circadian rhythms, energy homeostasis, neurodevelopment, and immune function. Both genetic polymorphisms in RORA and alterations in its expression levels have been closely associated with an increased susceptibility to depressive disorders [44–46]. As a core clock protein, functional disruptions in ROR α can directly impair the regulation of circadian rhythms, thereby increasing the risk for developing depressive disorders [47–49]. Moreover, ROR α participates in the regulation of neurogenesis and neuroplasticity through modulating the expression of crucial molecules such as BDNF and 5-HT, processes that are intimately linked to the neurobiological underpinnings of MDD [50, 51].

Recent studies have also uncovered a potential role for ROR α in influencing inflammation-associated processes relevant to MDD through its immunomodulatory functions [52, 53]. In summary, the four genes ABCC2, APP, HK2, and RORA are respectively involved in crucial molecular events and physiological processes intimately linked to the pathogenesis of depressive disorders, including neurotransmitter transport, amyloid metabolism, energy dysregulation, and circadian disruption. Their aberrant expression patterns provide potential biomarkers for the precise diagnosis of depression and evaluation of its severity. A comprehensive understanding of the multifaceted roles played by these biomarkers in governing diurnal rhythmicity, neuroplasticity, and mood homeostasis will shed light on the underlying biological pathways implicated in depressive symptomatology and inform the development of integrated therapeutic approaches.

Notably, the analysis of immune cell infiltration in blood samples revealed distinct alterations in MDD patients compared to healthy controls. This finding was consistent with a previous report in the field [52]. Specifically, Neutrophils were significantly increased, while memory B cells, CD8+ T cells, and resting Dendritic cells were significantly decreased in MDD patients. The increased infiltration of Neutrophils, a pro-inflammatory cell type, in MDD blood samples is consistent with the growing body of evidence linking neuroinflammation and immune dysregulation to the pathogenesis of depressive disorders [53]. Conversely, the reduced levels of memory B cells, CD8+ T cells, and resting Dendritic cells suggest a potential impairment in adaptive immune responses and antigen presentation in MDD patients [54, 55]. These findings align with previous reports of altered lymphocyte and antigen-presenting cell populations in depression [56]. Importantly, the correlation analyses between the 4 key CRGs and the infiltration levels of immune cell populations provide valuable insights into the potential mechanisms linking circadian rhythm disturbances and immune dysregulation in MDD. For instance, the strong positive correlation between RORA and the infiltration of CD8+ T cells and Monocytes suggests that RORA may play a pivotal role in regulating the anti-inflammatory functions of these immune cell types [57, 58]. Conversely, the negative correlations between RORA and Neutrophils, as well as naive CD4+ T cells, indicate that disruption of RORA-mediated circadian control could contribute to the pro-inflammatory state observed in MDD.

Importantly, the observed correlations between the 4 key CRGs and the infiltration levels of specific immune cell populations, such as neutrophils, T cells, and NK

cells, suggest a potential mechanistic link between circadian rhythm disruption and immune dysregulation in MDD. This finding is consistent with growing evidence supporting the critical role of neuroimmune system imbalances in the development and progression of depressive disorders [59]. However, in contrast to previous studies that have primarily focused on individual circadian genes or immune markers [60, 61], the present work has uniquely identified a panel of CRGs that are closely associated with both circadian and immune perturbations in MDD. Similarly, the positive associations between ABCC2, APP, and HK2 with the infiltration of Neutrophils and activated NK cells, coupled with the negative correlations with CD8+ T cells and Monocytes, imply that dysregulation of these CRGs may impair the balance between pro-inflammatory and anti-inflammatory immune responses in MDD. These findings build upon the growing body of evidence highlighting the critical role of the brain-immune axis in the pathophysiology of depressive disorders [62]. The present study's identification of a panel of key CRGs and their associations with specific immune cell populations represents a significant advancement compared to previous research that has primarily focused on individual circadian genes or immune markers. These findings provide a more comprehensive understanding of the complex interplay between disrupted circadian rhythms and immune dysregulation in MDD, and offer potential targets for the development of novel diagnostic and therapeutic strategies.

Most available antidepressants nowadays work through monoamine mechanisms [63]. To effectively explore drugs targeting key CRGs, this study performed screening, prediction and analysis of antidepressant drugs for 4 key CRGs, and obtained some referable results including melatonin and citalopram. Melatonin or melatonin receptor agonists are currently the main and effective drugs for regulating circadian rhythm disorders in MDD [64]. Agomelatine, the first approved antidepressant targeting melatonin receptors, significantly improved sleep quality and reduced waking in patients [65]. Citalopram, a selective serotonin reuptake inhibitor, is increasingly used for MDD treatment. It has the advantage of a rapid onset of action and exerts a significant antidepressant effect by modulating multiple neurotransmitters, including dopamine, GABA, and norepinephrine [66, 67]. In addition, we also screened some natural products from plants such as ferulic acid and isochlorogenic acid B. Ferulic acid has been proven to produce significant antidepressant effects in animal models of MDD through various mechanisms, providing a solid basis for its clinical application [68]. Ferulic acid can significantly improve APP deposition-induced neurofunctional impairments by activating the

PI3K/Akt signaling pathway [69]. Isochlorogenic acid B, abundant in plants like honeysuckle, chrysanthemum leaves, propolis, was found to have good effects on improving MDD and neuroinflammation. Its mechanism is associated with regulating brain-derived neurotrophic factor signaling pathways [70]. More data are needed to support the direct effects of alternative drugs on MDD.

In summary, this integrative study revealed four key circadian rhythm genes (ABCC2, APP, HK2, and RORA) that are closely associated with MDD pathogenesis and may serve as promising diagnostic biomarkers and therapeutic targets. The identified genes were found to be functionally involved in circadian rhythm regulation, neuronal processes, immune responses, and metabolic pathways implicated in MDD. Additionally, these genes showed significant correlations with immune cell infiltration profiles, highlighting the potential contribution of circadian rhythm disruption and neuroinflammation to MDD etiology. Furthermore, we predicted several small molecule compounds that could directly target these circadian proteins, providing a foundation for future drug development efforts. Collectively, our findings shed new light on the intricate relationships between circadian rhythms, immune dysregulation, and MDD pathophysiology, paving the way for more effective diagnosis, prevention, and treatment strategies for this debilitating disorder.

Looking ahead, further experimental validation of the identified circadian biomarkers and their functional roles in MDD pathogenesis is warranted. Additionally, preclinical and clinical studies are needed to evaluate the therapeutic potential of the predicted circadian rhythm-modulating compounds for MDD treatment. Given the multifaceted nature of MDD, a combinatorial approach targeting multiple circadian genes and pathways may be required for optimal therapeutic efficacy. Furthermore, integration of circadian rhythm monitoring and chronotherapeutic interventions into existing treatment paradigms could enhance the personalization and precision of MDD management. By elucidating the complex interplay between circadian rhythms, neurobiological processes, and environmental factors in MDD, we can pave the way for more holistic and tailored strategies to alleviate the substantial burden imposed by this prevalent mental health disorder.

AUTHOR CONTRIBUTIONS

YHS and QZT conceived and designed the study. YHS and JZ wrote the manuscript. CWH and XLL analyzed the data and performed the statistical analysis. YHS and XDL contributed to the literature search and preparation of figures and tables. QZT supervised the study. All authors have read and approved the final manuscript.

CONFLICTS OF INTEREST

The authors declare no conflicts of interest related to this study.

ETHICAL STATEMENT

No human or animal subjects were directly involved in this study. All data were obtained from public databases and therefore, ethical approval is not required for this study.

FUNDING

This work was supported by the Hunan Provincial Natural Science Foundation (No. 2023JJ60127) and Graduate Student Innovation Program Grant (No. 2023CX03) from Hunan University of Traditional Medicine.

REFERENCES

1. Park LT, Zarate CA Jr. Depression in the Primary Care Setting. *N Engl J Med*. 2019; 380:559–68. <https://doi.org/10.1056/NEJMcp1712493> PMID:30726688
2. Beurel E, Toups M, Nemeroff CB. The Bidirectional Relationship of Depression and Inflammation: Double Trouble. *Neuron*. 2020; 107:234–56. <https://doi.org/10.1016/j.neuron.2020.06.002> PMID:32553197
3. McGrath JJ, Al-Hamzawi A, Alonso J, Altwaijri Y, Andrade LH, Bromet EJ, Bruffaerts R, de Almeida JMC, Chardoul S, Chiu WT, Degenhardt L, Demler OV, Ferry F, et al, and WHO World Mental Health Survey Collaborators. Age of onset and cumulative risk of mental disorders: a cross-national analysis of population surveys from 29 countries. *Lancet Psychiatry*. 2023; 10:668–81. [https://doi.org/10.1016/S2215-0366\(23\)00193-1](https://doi.org/10.1016/S2215-0366(23)00193-1) PMID:37531964
4. Kuehner C. Why is depression more common among women than among men? *Lancet Psychiatry*. 2017; 4:146–58. [https://doi.org/10.1016/S2215-0366\(16\)30263-2](https://doi.org/10.1016/S2215-0366(16)30263-2) PMID:27856392
5. Jiao H, Yang H, Yan Z, Chen J, Xu M, Jiang Y, Liu Y, Xue Z, Ma Q, Li X, Chen J. Traditional Chinese Formula Xiaoyaosan Alleviates Depressive-Like Behavior in CUMS Mice by Regulating PEBP1-GPX4-Mediated Ferroptosis in the Hippocampus. *Neuropsychiatr Dis Treat*. 2021; 17:1001–19. <https://doi.org/10.2147/NDT.S302443> PMID:33854318

6. Furukawa TA, Cipriani A, Cowen PJ, Leucht S, Egger M, Salanti G. Optimal dose of selective serotonin reuptake inhibitors, venlafaxine, and mirtazapine in major depression: a systematic review and dose-response meta-analysis. *Lancet Psychiatry*. 2019; 6:601–9. [https://doi.org/10.1016/S2215-0366\(19\)30217-2](https://doi.org/10.1016/S2215-0366(19)30217-2) PMID:[31178367](https://pubmed.ncbi.nlm.nih.gov/31178367/)
7. Garay RP, Zarate CA Jr, Charpeaud T, Citrome L, Correll CU, Hameg A, Llorca PM. Investigational drugs in recent clinical trials for treatment-resistant depression. *Expert Rev Neurother*. 2017; 17:593–609. <https://doi.org/10.1080/14737175.2017.1283217> PMID:[28092469](https://pubmed.ncbi.nlm.nih.gov/28092469/)
8. Nedic Erjavec G, Sagud M, Nikolac Perkovic M, Svob Strac D, Konjevod M, Tudor L, Uzun S, Pivac N. Depression: Biological markers and treatment. *Prog Neuropsychopharmacol Biol Psychiatry*. 2021; 105:110139. <https://doi.org/10.1016/j.pnpbp.2020.110139> PMID:[33068682](https://pubmed.ncbi.nlm.nih.gov/33068682/)
9. Martinowich K, Manji H, Lu B. New insights into BDNF function in depression and anxiety. *Nat Neurosci*. 2007; 10:1089–93. <https://doi.org/10.1038/nn1971> PMID:[17726474](https://pubmed.ncbi.nlm.nih.gov/17726474/)
10. Neves AR, Albuquerque T, Quintela T, Costa D. Circadian rhythm and disease: Relationship, new insights, and future perspectives. *J Cell Physiol*. 2022; 237:3239–56. <https://doi.org/10.1002/jcp.30815> PMID:[35696609](https://pubmed.ncbi.nlm.nih.gov/35696609/)
11. Pandi-Perumal SR, Monti JM, Burman D, Karthikeyan R, BaHammam AS, Spence DW, Brown GM, Narashimhan M. Clarifying the role of sleep in depression: A narrative review. *Psychiatry Res*. 2020; 291:113239. <https://doi.org/10.1016/j.psychres.2020.113239> PMID:[32593854](https://pubmed.ncbi.nlm.nih.gov/32593854/)
12. Dollish HK, Tsyglakova M, McClung CA. Circadian rhythms and mood disorders: Time to see the light. *Neuron*. 2024; 112:25–40. <https://doi.org/10.1016/j.neuron.2023.09.023> PMID:[37858331](https://pubmed.ncbi.nlm.nih.gov/37858331/)
13. Wirz-Justice A. Biological rhythm disturbances in mood disorders. *Int Clin Psychopharmacol*. 2006 (Suppl 1); 21:S11–5. <https://doi.org/10.1097/01.yic.0000195660.37267.cf> PMID:[16436934](https://pubmed.ncbi.nlm.nih.gov/16436934/)
14. Qiu P, Jiang J, Liu Z, Cai Y, Huang T, Wang Y, Liu Q, Nie Y, Liu F, Cheng J, Li Q, Tang YC, Poo MM, et al. BMAL1 knockout macaque monkeys display reduced sleep and psychiatric disorders. *Natl Sci Rev*. 2019; 6:87–100. <https://doi.org/10.1093/nsr/nwz002> PMID:[34691834](https://pubmed.ncbi.nlm.nih.gov/34691834/)
15. Zhou TT, Sun JJ, Tang LD, Yuan Y, Wang JY, Zhang L. Potential diagnostic markers and therapeutic targets for rheumatoid arthritis with comorbid depression based on bioinformatics analysis. *Front Immunol*. 2023; 14:1007624. <https://doi.org/10.3389/fimmu.2023.1007624> PMID:[36911710](https://pubmed.ncbi.nlm.nih.gov/36911710/)
16. Newman AM, Steen CB, Liu CL, Gentles AJ, Chaudhuri AA, Scherer F, Khodadoust MS, Esfahani MS, Luca BA, Steiner D, Diehn M, Alizadeh AA. Determining cell type abundance and expression from bulk tissues with digital cytometry. *Nat Biotechnol*. 2019; 37:773–82. <https://doi.org/10.1038/s41587-019-0114-2> PMID:[31061481](https://pubmed.ncbi.nlm.nih.gov/31061481/)
17. Freshour SL, Kiwala S, Cotto KC, Coffman AC, McMichael JF, Song JJ, Griffith M, Griffith OL, Wagner AH. Integration of the Drug-Gene Interaction Database (DGIdb 4.0) with open crowdsource efforts. *Nucleic Acids Res*. 2021; 49:D1144–51. <https://doi.org/10.1093/nar/gkaa1084> PMID:[33237278](https://pubmed.ncbi.nlm.nih.gov/33237278/)
18. Gao Y, Kim S, Lee YI, Lee J. Cellular Stress-Modulating Drugs Can Potentially Be Identified by in Silico Screening with Connectivity Map (CMap). *Int J Mol Sci*. 2019; 20:5601. <https://doi.org/10.3390/ijms20225601> PMID:[31717493](https://pubmed.ncbi.nlm.nih.gov/31717493/)
19. COVID-19 Mental Disorders Collaborators. Global prevalence and burden of depressive and anxiety disorders in 204 countries and territories in 2020 due to the COVID-19 pandemic. *Lancet*. 2021; 398:1700–12. [https://doi.org/10.1016/S0140-6736\(21\)02143-7](https://doi.org/10.1016/S0140-6736(21)02143-7) PMID:[34634250](https://pubmed.ncbi.nlm.nih.gov/34634250/)
20. Liu L, Wang H, Chen X, Zhang Y, Zhang H, Xie P. Gut microbiota and its metabolites in depression: from pathogenesis to treatment. *EBioMedicine*. 2023; 90:104527. <https://doi.org/10.1016/j.ebiom.2023.104527> PMID:[36963238](https://pubmed.ncbi.nlm.nih.gov/36963238/)
21. Lopresti AL, Hood SD, Drummond PD. A review of lifestyle factors that contribute to important pathways associated with major depression: diet, sleep and exercise. *J Affect Disord*. 2013; 148:12–27. <https://doi.org/10.1016/j.jad.2013.01.014> PMID:[23415826](https://pubmed.ncbi.nlm.nih.gov/23415826/)
22. Li JZ, Bunney BG, Meng F, Hagenauer MH, Walsh DM, Vawter MP, Evans SJ, Choudary PV, Cartagena P,

- Barchas JD, Schatzberg AF, Jones EG, Myers RM, et al. Circadian patterns of gene expression in the human brain and disruption in major depressive disorder. *Proc Natl Acad Sci U S A*. 2013; 110:9950–5. <https://doi.org/10.1073/pnas.1305814110> PMID:[23671070](https://pubmed.ncbi.nlm.nih.gov/23671070/)
23. Otsuka T, Le HT, Thein ZL, Ihara H, Sato F, Nakao T, Kohsaka A. Deficiency of the circadian clock gene *Rev-erb α* induces mood disorder-like behaviours and dysregulation of the serotonergic system in mice. *Physiol Behav*. 2022; 256:113960. <https://doi.org/10.1016/j.physbeh.2022.113960> PMID:[36115382](https://pubmed.ncbi.nlm.nih.gov/36115382/)
24. Takeda Y, Jothi R, Birault V, Jetten AM. ROR γ directly regulates the circadian expression of clock genes and downstream targets in vivo. *Nucleic Acids Res*. 2012; 40:8519–35. <https://doi.org/10.1093/nar/gks630> PMID:[22753030](https://pubmed.ncbi.nlm.nih.gov/22753030/)
25. Akashi M, Takumi T. The orphan nuclear receptor ROR α regulates circadian transcription of the mammalian core-clock *Bmal1*. *Nat Struct Mol Biol*. 2005; 12:441–8. <https://doi.org/10.1038/nsmb925> PMID:[15821743](https://pubmed.ncbi.nlm.nih.gov/15821743/)
26. Gekakis N, Staknis D, Nguyen HB, Davis FC, Wilsbacher LD, King DP, Takahashi JS, Weitz CJ. Role of the CLOCK protein in the mammalian circadian mechanism. *Science*. 1998; 280:1564–9. <https://doi.org/10.1126/science.280.5369.1564> PMID:[9616112](https://pubmed.ncbi.nlm.nih.gov/9616112/)
27. Busino L, Bassermann F, Maiolica A, Lee C, Nolan PM, Godinho SI, Draetta GF, Pagano M. SCFF β 13 controls the oscillation of the circadian clock by directing the degradation of cryptochrome proteins. *Science*. 2007; 316:900–4. <https://doi.org/10.1126/science.1141194> PMID:[17463251](https://pubmed.ncbi.nlm.nih.gov/17463251/)
28. Bortolato B, Hyphantis TN, Valpione S, Perini G, Maes M, Morris G, Kubera M, Köhler CA, Fernandes BS, Stubbs B, Pavlidis N, Carvalho AF. Depression in cancer: The many biobehavioral pathways driving tumor progression. *Cancer Treat Rev*. 2017; 52:58–70. <https://doi.org/10.1016/j.ctrv.2016.11.004> PMID:[27894012](https://pubmed.ncbi.nlm.nih.gov/27894012/)
29. Christie J, Sharpley CF, Bitsika V, Christie D. Evidence of depression-associated circadian rhythm disruption and regret in prostate cancer patients after surgery. *Support Care Cancer*. 2017; 25:3603–5. <https://doi.org/10.1007/s00520-017-3913-3> PMID:[28980139](https://pubmed.ncbi.nlm.nih.gov/28980139/)
30. Dwyer JB, Aftab A, Radhakrishnan R, Widge A, Rodriguez CI, Carpenter LL, Nemeroff CB, McDonald WM, Kalin NH, and APA Council of Research Task Force on Novel Biomarkers and Treatments. Hormonal Treatments for Major Depressive Disorder: State of the Art. *Am J Psychiatry*. 2020; 177:686–705. <https://doi.org/10.1176/appi.ajp.2020.19080848> PMID:[32456504](https://pubmed.ncbi.nlm.nih.gov/32456504/)
31. Vagnerová K, Ergang P, Soták M, Balounová K, Kvapilová P, Vodička M, Pácha J. Diurnal expression of ABC and SLC transporters in jejunum is modulated by adrenalectomy. *Comp Biochem Physiol C Toxicol Pharmacol*. 2019; 226:108607. <https://doi.org/10.1016/j.cbpc.2019.108607> PMID:[31422161](https://pubmed.ncbi.nlm.nih.gov/31422161/)
32. Gachon F, Firsov D. The role of circadian timing system on drug metabolism and detoxification. *Expert Opin Drug Metab Toxicol*. 2011; 7:147–58. <https://doi.org/10.1517/17425255.2011.544251> PMID:[21192771](https://pubmed.ncbi.nlm.nih.gov/21192771/)
33. Cacabelos R, Carril JC, Corzo L, Pego R, Cacabelos N, Alcaraz M, Muñiz A, Martínez-Iglesias O, Naidoo V. Pharmacogenetics of anxiety and depression in Alzheimer's disease. *Pharmacogenomics*. 2023; 24:27–57. <https://doi.org/10.2217/pgs-2022-0137> PMID:[36628952](https://pubmed.ncbi.nlm.nih.gov/36628952/)
34. Shao YY, Huang J, Ma YR, Han M, Ma K, Qin HY, Rao Z, Wu XA. Serum serotonin reduced the expression of hepatic transporter Mrp2 and P-gp via regulating nuclear receptor CAR in PI-IBS rats. *Can J Physiol Pharmacol*. 2015; 93:633–9. <https://doi.org/10.1139/cjpp-2015-0039> PMID:[26053941](https://pubmed.ncbi.nlm.nih.gov/26053941/)
35. Pułaski L, Kania K, Ratajewski M, Uchiumi T, Kuwano M, Bartosz G. Differential regulation of the human MRP2 and MRP3 gene expression by glucocorticoids. *J Steroid Biochem Mol Biol*. 2005; 96:229–34. <https://doi.org/10.1016/j.jsbmb.2005.03.004> PMID:[15979871](https://pubmed.ncbi.nlm.nih.gov/15979871/)
36. Song H, Moon M, Choe HK, Han DH, Jang C, Kim A, Cho S, Kim K, Mook-Jung I. A β -induced degradation of BMAL1 and CBP leads to circadian rhythm disruption in Alzheimer's disease. *Mol Neurodegener*. 2015; 10:13. <https://doi.org/10.1186/s13024-015-0007-x> PMID:[25888034](https://pubmed.ncbi.nlm.nih.gov/25888034/)
37. Niu L, Zhang F, Xu X, Yang Y, Li S, Liu H, Le W. Chronic sleep deprivation altered the expression of circadian clock genes and aggravated Alzheimer's disease neuropathology. *Brain Pathol*. 2022; 32:e13028. <https://doi.org/10.1111/bpa.13028>

PMID:[34668266](https://pubmed.ncbi.nlm.nih.gov/34668266/)

38. Harerimana NV, Liu Y, Gerasimov ES, Duong D, Beach TG, Reiman EM, Schneider JA, Boyle P, Lori A, Bennett DA, Lah JJ, Levey AI, Seyfried NT, et al. Genetic Evidence Supporting a Causal Role of Depression in Alzheimer's Disease. *Biol Psychiatry*. 2022; 92:25–33.
<https://doi.org/10.1016/j.biopsych.2021.11.025>
PMID:[35177243](https://pubmed.ncbi.nlm.nih.gov/35177243/)
39. Huang YY, Gan YH, Yang L, Cheng W, Yu JT. Depression in Alzheimer's Disease: Epidemiology, Mechanisms, and Treatment. *Biol Psychiatry*. 2024; 95:992–1005.
<https://doi.org/10.1016/j.biopsych.2023.10.008>
PMID:[37866486](https://pubmed.ncbi.nlm.nih.gov/37866486/)
40. Al-Kuraishy HM, Jabir MS, Al-Gareeb AI, Albuhadily AK, Albukhaty S, Sulaiman GM, Batiha GE. Evaluation and targeting of amyloid precursor protein (APP)/amyloid beta (A β) axis in amyloidogenic and non-amyloidogenic pathways: A time outside the tunnel. *Ageing Res Rev*. 2023; 92:102119.
<https://doi.org/10.1016/j.arr.2023.102119>
PMID:[37931848](https://pubmed.ncbi.nlm.nih.gov/37931848/)
41. Wu X, Shen Q, Chang H, Li J, Xing D. Promoted CD4⁺ T cell-derived IFN- γ /IL-10 by photobiomodulation therapy modulates neurogenesis to ameliorate cognitive deficits in APP/PS1 and 3xTg-AD mice. *J Neuroinflammation*. 2022; 19:253.
<https://doi.org/10.1186/s12974-022-02617-5>
PMID:[36217178](https://pubmed.ncbi.nlm.nih.gov/36217178/)
42. Singh G, Storey KB. MondoA:MLX complex regulates glucose-dependent gene expression and links to circadian rhythm in liver and brain of the freeze-tolerant wood frog, *Rana sylvatica*. *Mol Cell Biochem*. 2020; 473:203–16.
<https://doi.org/10.1007/s11010-020-03820-9>
PMID:[32638259](https://pubmed.ncbi.nlm.nih.gov/32638259/)
43. Harfmann BD, Schroder EA, Kachman MT, Hodge BA, Zhang X, Esser KA. Muscle-specific loss of Bmal1 leads to disrupted tissue glucose metabolism and systemic glucose homeostasis. *Skelet Muscle*. 2016; 6:12.
<https://doi.org/10.1186/s13395-016-0082-x>
PMID:[27486508](https://pubmed.ncbi.nlm.nih.gov/27486508/)
44. Terracciano A, Tanaka T, Sutin AR, Sanna S, Deiana B, Lai S, Uda M, Schlessinger D, Abecasis GR, Ferrucci L, Costa PT Jr. Genome-wide association scan of trait depression. *Biol Psychiatry*. 2010; 68:811–7.
<https://doi.org/10.1016/j.biopsych.2010.06.030>
PMID:[20800221](https://pubmed.ncbi.nlm.nih.gov/20800221/)
45. Ming Q, Wang X, Chai Q, Yi J, Yao S. Retinoid-related orphan receptor alpha (RORA) gene variation is associated with trait depression. *Psychiatry Res*. 2015; 229:629–30.
<https://doi.org/10.1016/j.psychres.2015.07.014>
PMID:[26184991](https://pubmed.ncbi.nlm.nih.gov/26184991/)
46. Chen Z, Tao S, Zhu R, Tian S, Sun Y, Wang H, Yan R, Shao J, Zhang Y, Zhang J, Yao Z, Lu Q. Aberrant functional connectivity between the suprachiasmatic nucleus and the superior temporal gyrus: Bridging RORA gene polymorphism with diurnal mood variation in major depressive disorder. *J Psychiatr Res*. 2021; 132:123–30.
<https://doi.org/10.1016/j.jpsychires.2020.09.037>
PMID:[33091686](https://pubmed.ncbi.nlm.nih.gov/33091686/)
47. Sato TK, Panda S, Miraglia LJ, Reyes TM, Rudic RD, McNamara P, Naik KA, FitzGerald GA, Kay SA, Hogenesch JB. A functional genomics strategy reveals Rora as a component of the mammalian circadian clock. *Neuron*. 2004; 43:527–37.
<https://doi.org/10.1016/j.neuron.2004.07.018>
PMID:[15312651](https://pubmed.ncbi.nlm.nih.gov/15312651/)
48. Maglione JE, Nievergelt CM, Parimi N, Evans DS, Ancoli-Israel S, Stone KL, Yaffe K, Redline S, Tranah GJ, and Study of Osteoporotic Fractures in Women (SOF) and Osteoporotic Fractures in Men Study (MrOS) Research Groups. Associations of PER3 and RORA Circadian Gene Polymorphisms and Depressive Symptoms in Older Adults. *Am J Geriatr Psychiatry*. 2015; 23:1075–87.
<https://doi.org/10.1016/j.jagp.2015.03.002>
PMID:[25892098](https://pubmed.ncbi.nlm.nih.gov/25892098/)
49. Hennings JM, Uhr M, Klengel T, Weber P, Pütz B, Touma C, Czamara D, Ising M, Holsboer F, Lucae S. RNA expression profiling in depressed patients suggests retinoid-related orphan receptor alpha as a biomarker for antidepressant response. *Transl Psychiatry*. 2015; 5:e538.
<https://doi.org/10.1038/tp.2015.9>
PMID:[25826113](https://pubmed.ncbi.nlm.nih.gov/25826113/)
50. Rozenblit-Susan S, Chapnik N, Froy O. Serotonin Prevents Differentiation of Brown Adipocytes by Interfering with Their Clock. *Obesity (Silver Spring)*. 2019; 27:2018–24.
<https://doi.org/10.1002/oby.22606>
PMID:[31674727](https://pubmed.ncbi.nlm.nih.gov/31674727/)
51. Koibuchi N, Yamaoka S, Chin WW. Effect of altered thyroid status on neurotrophin gene expression during postnatal development of the mouse cerebellum. *Thyroid*. 2001; 11:205–10.
<https://doi.org/10.1089/105072501750159534>
PMID:[11327610](https://pubmed.ncbi.nlm.nih.gov/11327610/)
52. Han S, Li Z, Han F, Jia Y, Qi L, Wu G, Cai W, Xu Y, Li C, Zhang W, Hu D. ROR alpha protects against LPS-induced inflammation by down-regulating SIRT1/NF-kappa B pathway. *Arch Biochem Biophys*. 2019;

- 668:1–8.
<https://doi.org/10.1016/j.abb.2019.05.003>
PMID:[31071300](https://pubmed.ncbi.nlm.nih.gov/31071300/)
53. Sforzini L, Cattaneo A, Ferrari C, Turner L, Mariani N, Enache D, Hastings C, Lombardo G, Nettis MA, Nikkheslat N, Worrell C, Zajkowska Z, Kose M, et al, and Neuroimmunology of Mood Disorders and Alzheimer's Disease (NIMA) Consortium. Higher immune-related gene expression in major depression is independent of CRP levels: results from the BIODEP study. *Transl Psychiatry*. 2023; 13:185.
<https://doi.org/10.1038/s41398-023-02438-x>
PMID:[37264010](https://pubmed.ncbi.nlm.nih.gov/37264010/)
54. Su M, Ouyang X, Song Y. Neutrophil to lymphocyte ratio, platelet to lymphocyte ratio, and monocyte to lymphocyte ratio in depression: A meta-analysis. *J Affect Disord*. 2022; 308:375–83.
<https://doi.org/10.1016/j.jad.2022.04.038>
PMID:[35439466](https://pubmed.ncbi.nlm.nih.gov/35439466/)
55. Miller AH. Depression and immunity: a role for T cells? *Brain Behav Immun*. 2010; 24:1–8.
<https://doi.org/10.1016/j.bbi.2009.09.009>
PMID:[19818725](https://pubmed.ncbi.nlm.nih.gov/19818725/)
56. Bauer ME, Papadopoulos A, Poon L, Perks P, Lightman SL, Checkley S, Shanks N. Dexamethasone-induced effects on lymphocyte distribution and expression of adhesion molecules in treatment-resistant depression. *Psychiatry Res*. 2002; 113:1–15.
[https://doi.org/10.1016/s0165-1781\(02\)00243-3](https://doi.org/10.1016/s0165-1781(02)00243-3)
PMID:[12467941](https://pubmed.ncbi.nlm.nih.gov/12467941/)
57. Pozo D, García-Mauriño S, Guerrero JM, Calvo JR. mRNA expression of nuclear receptor RZR/RORalpha, melatonin membrane receptor MT, and hydroxindole-O-methyltransferase in different populations of human immune cells. *J Pineal Res*. 2004; 37:48–54.
<https://doi.org/10.1111/j.1600-079X.2004.00135.x>
PMID:[15230868](https://pubmed.ncbi.nlm.nih.gov/15230868/)
58. Hams E, Roberts J, Bermingham R, Hogan AE, O'Shea D, O'Neill L, Fallon PG. Role for Retinoic Acid-Related Orphan Receptor Alpha (ROR α) Expressing Macrophages in Diet-Induced Obesity. *Front Immunol*. 2020; 11:1966.
<https://doi.org/10.3389/fimmu.2020.01966>
PMID:[32973801](https://pubmed.ncbi.nlm.nih.gov/32973801/)
59. Hodes GE, Kana V, Menard C, Merad M, Russo SJ. Neuroimmune mechanisms of depression. *Nat Neurosci*. 2015; 18:1386–93.
<https://doi.org/10.1038/nn.4113>
PMID:[26404713](https://pubmed.ncbi.nlm.nih.gov/26404713/)
60. Brasanac J, Ramien C, Gamradt S, Taenzer A, Glau L, Ritter K, Patas K, Agorastos A, Wiedemann K, Demiralay C, Fischer F, Otte C, Bellmann-Strobl J, et al. Immune signature of multiple sclerosis-associated depression. *Brain Behav Immun*. 2022; 100:174–82.
<https://doi.org/10.1016/j.bbi.2021.11.022>
PMID:[34863857](https://pubmed.ncbi.nlm.nih.gov/34863857/)
61. Daut RA, Fonken LK. Circadian regulation of depression: A role for serotonin. *Front Neuroendocrinol*. 2019; 54:100746.
<https://doi.org/10.1016/j.yfrne.2019.04.003>
PMID:[31002895](https://pubmed.ncbi.nlm.nih.gov/31002895/)
62. Zhou B, Zhu Z, Ransom BR, Tong X. Oligodendrocyte lineage cells and depression. *Mol Psychiatry*. 2021; 26:103–17.
<https://doi.org/10.1038/s41380-020-00930-0>
PMID:[33144710](https://pubmed.ncbi.nlm.nih.gov/33144710/)
63. de Bodinat C, Guardiola-Lemaitre B, Mocaër E, Renard P, Muñoz C, Millan MJ. Agomelatine, the first melatonergic antidepressant: discovery, characterization and development. *Nat Rev Drug Discov*. 2010; 9:628–42.
<https://doi.org/10.1038/nrd3140>
PMID:[20577266](https://pubmed.ncbi.nlm.nih.gov/20577266/)
64. Stein RM, Kang HJ, McCorvy JD, Glatfelter GC, Jones AJ, Che T, Slocum S, Huang XP, Savych O, Moroz YS, Stauch B, Johansson LC, Cherezov V, et al. Virtual discovery of melatonin receptor ligands to modulate circadian rhythms. *Nature*. 2020; 579:609–14.
<https://doi.org/10.1038/s41586-020-2027-0>
PMID:[32040955](https://pubmed.ncbi.nlm.nih.gov/32040955/)
65. Hickie IB, Rogers NL. Novel melatonin-based therapies: potential advances in the treatment of major depression. *Lancet*. 2011; 378:621–31.
[https://doi.org/10.1016/S0140-6736\(11\)60095-0](https://doi.org/10.1016/S0140-6736(11)60095-0)
PMID:[21596429](https://pubmed.ncbi.nlm.nih.gov/21596429/)
66. Pastoor D, Gobburu J. Clinical pharmacology review of escitalopram for the treatment of depression. *Expert Opin Drug Metab Toxicol*. 2014; 10:121–8.
<https://doi.org/10.1517/17425255.2014.863873>
PMID:[24289655](https://pubmed.ncbi.nlm.nih.gov/24289655/)
67. Bhattacharyya S, Ahmed AT, Arnold M, Liu D, Luo C, Zhu H, Mahmoudiandehkordi S, Neavin D, Louie G, Dunlop BW, Frye MA, Wang L, Weinsilboum RM, et al. Metabolomic signature of exposure and response to citalopram/escitalopram in depressed outpatients. *Transl Psychiatry*. 2019; 9:173.
<https://doi.org/10.1038/s41398-019-0507-5>
PMID:[31273200](https://pubmed.ncbi.nlm.nih.gov/31273200/)
68. Dong X, Zhao D. Ferulic acid as a therapeutic agent in depression: Evidence from preclinical studies. *CNS Neurosci Ther*. 2023; 29:2397–412.
<https://doi.org/10.1111/cns.14265>
PMID:[37183361](https://pubmed.ncbi.nlm.nih.gov/37183361/)

69. Wang NY, Li JN, Liu WL, Huang Q, Li WX, Tan YH, Liu F, Song ZH, Wang MY, Xie N, Mao RR, Gan P, Ding YQ, et al. Ferulic Acid Ameliorates Alzheimer's Disease-like Pathology and Repairs Cognitive Decline by Preventing Capillary Hypofunction in APP/PS1 Mice. *Neurotherapeutics*. 2021; 18:1064–80. <https://doi.org/10.1007/s13311-021-01024-7> PMID:[33786807](https://pubmed.ncbi.nlm.nih.gov/33786807/)
70. Shi JX, Cheng C, Ruan HN, Li J, Liu CM. Isochlorogenic acid B alleviates lead-induced anxiety, depression and neuroinflammation in mice by the BDNF pathway. *Neurotoxicology*. 2023; 98:1–8. <https://doi.org/10.1016/j.neuro.2023.06.007> PMID:[37385299](https://pubmed.ncbi.nlm.nih.gov/37385299/)

SUPPLEMENTARY MATERIALS

Supplementary Table

Supplementary Table 1. 1475 circadian rhythm genes (CRGs) collected from the MSigDB database.

SLC2A2	SUMO3	SYNCRIP	CCT7	CCNE1	CSMD1	PPARGC1A	DDIT3	CBL	CREB3L3	KMT2D	PI4KA
RBP2	GPR176	PDZD3	SSB	DICER1	ATM	TNFRSF11A	ATF3	TSC2	TRH	NAT2	SLC2A3
MEF2D	PSMC4	AVPR1A	RAB5B	PEMT	CYP2E1	EPHB2	CEBPG	SPRY2	DGKQ	DIO3	ADCY3
CLOCK	ATF2	MAX	SMCHD1	RGS20	VRK2	PTCH1	NPAS3	GATD3	MPO	ICAM1	APRT
PER2	APP	CRTC2	TAGLN2	PGR	PSMB1	NEUROD1	IL4	CYP3A4	SULT2A1	CAVIN2	BCKDK
PER3	FDFT1	CRTC3	RAB1A	XPA	PSMD12	TRIM35	PNPLA3	MED9	TELO2	SULT1A1	CYP7B1
PER1	PDE6B	TDRKH	HNRNPH3	SLC12A2	RHOA	NCOR2	USP30	SEM1	EHMT2	FABP4	ENO2
CRY1	SUGP1	RGS16	AHNAK	SLC5A1	GSR	MYBBP1A	DDC	BRINP1	CDK6	IL6R	HPRT1
ARNTL	THBS1	GNAQ	EIF3E	NUP98	OLFML3	CSNK1A1L	MEF2A	BLMH	IKBKB	ADRA2C	PDK1
CRY2	ACADS	TH	RALY	RAE1	RB1	MIF	GUSB	GRM5	TPO	UCP2	SUCLA2
TIMELESS	CLTC	H2BC11	AURKAIP1	NPSR1	GCK	HTR1B	KDM1A	ARID1A	NMNAT1	WEE1	ATIC
NPAS2	PLCB4	SUV39H1	APMAP	HELLS	ABC7	CALCA	SRD5A1	RABGEF1	ABCC3	EGFR	CTPS1
ARNTL2	GLO1	PRMT1	MAGEC1	IMMT	ANGPTL2	MAPK3	DRD3	RAP1GAP	PKLR	CYP1A1	FDXR
CIPC	TIPIN	RPS19	CPNE9	SUV39H2	SNCA	TRIP12	PTGDR	KCNQ1	INPP5D	CALB2	GNAI1
CSNK1D	PPP2R1B	HMGA1	HID1	CH13L1	JAK2	TERT	ARRB1	FOSB	PFKP	HDC	GNAI2
NR1D1	PRKDC	RPL36	SEPTIN7	MAFK	NR1H3	TNPO1	CYP11B2	GADD45A	PIK3R5	CDK2	GPT2
CSNK1E	PRNP	RPL39	ADAR	APC	ESRRB	PRKN	MRE11	TUBA1B	ACSF3	ARF1	HSD17B4
CIART	SREBF1	APOE	USF1	TF	CAMK1	LEMD3	GLUL	ABHD5	IRF4	GUCA2B	ITPR3
BHLHE40	ENOX2	KAT8	ERN1	MMP3	NCAM1	UCHL5	PIK3C2A	HS3ST2	MECR	DUSP4	RAD21
BHLHE41	SLC41A1	ADRB1	CDKN2A	COPA	ATG14	TBL3	PPOX	XBPI	PANK2	CYP1B1	SMC3
RORA	TBL1X	CBX3	UBR5	SERPINF2	H2BC15	UBE2O	PCNA	NFE2	HAS3	FADS1	CHD2
DBP	GRP	GPI	ZBTB17	STAR	AQP3	COPS6	BAX	HMGCR	B4GALT2	CDC25A	ENPP2
PASD1	PPAT	LEPR	ATG7	MITF	SPSB1	ZNF207	ADRB2	ANKK1	CIDEC	JUNB	PCBD1
NOCT	XPO1	ZNF44	TRAF2	GSTP1	RPA2	LOC102724428	XDH	HEBP1	FFAR1	FBXO31	PFKFB3
AANAT	SPR	PSME2	ORMDL3	PIK3R2	MAOA	ZNF174	RPL3	CYP11B1	BRWD1	CLSPN	VAPB
NR1D2	HAT1	METTL14	CES1	PEBP1	FHIT	USP38	PSME4	FABP7	SERINC1	EGF	CTBP2
FBXL3	RACK1	COPS2	BGLAP	ABC7	CHRM3	OGG1	HUS1	DCP2	DHX29	FBXL14	EBP
SIRT1	TGS1	MAPK14	HES1	GIP	NECTIN1	KCNC2	PRDX6	SIM1	SLC25A27	ADK	EMD
NFIL3	CHD9	CS	NPY2R	EPO	THPO	AHRR	SYP	MT2A	SRPRB	CYP17A1	GATAD2B
RAI1	HELZ2	PPP2R5D	HRAS	IFNA1	RYR2	CDKN1B	IGF1R	CHD4	FUT5	FBP1	HDAC10
GSK3B	RASD1	HSPA5	AGRP	SLC9A3	AR	PBRM1	RRAS2	CEBPE	KCNG2	IDS	PI4KB
OPN4	KITLG	ZBP2	SHBG	PPP2CA	GGT1	CST3	EPB41	MTAP	YTHDC1	CACNA1A	PTPN13
BTRC	HBB	HSF1	CDKN1A	ATR	NR1I2	ADORA2A	GRM7	AFP	EXOSC4	GLDC	SDC4
NR3C1	EPAS1	P4HB	RPS2	MT1F	NR6A1	PRKG1	HABP2	GAPVD1	ENY2	ACACB	SDHD
CREBBP	NFKB2	ALDOA	ARNT2	FOXP3	MAGEC2	STX1A	PRKCB	RHOD	H1-5	AK1	GNB2
CSNK2A1	LRPPRC	TLN1	ADCY1	TLR4	TAC1	TAB2	TRPA1	ITGB1	KMT5B	AKR1B1	GNB4
HDAC3	HSPA8	PDIA6	NAGLU	SLC6A3	GPT	GFRA1	CBLB	PRKCD	MTARC2	HADHB	SULT1A2
TP53	DNAJA1	HSPA1A	NOS1	HBA1	SLC46A1	PURA	FANCL	ADSL	DUSP6	LBR	TINF2
PPARA	MAGED1	FOXO1	MAP2K7	CELF2	FGF21	EIF4G2	GRIK1	ALDH6A1	CXCL8	ADD1	BAZ1B
ID2	WDR5	NCL	PRKAA2	CNP	RPS6KA1	MYF6	PTPRT	ADCY8	HSPA4	RBP4	CUL7
EP300	AF2	SST	SLC2A1	TUBB	DNAH8	PRKAR1A	QKI	CA14	HTR3A	SULT2B1	EBF1
NCOA2	CEBPA	CCL2	SLC16A1	YWHAB	CCL4	BTG1	ATRIP	CYP51A1	H3-3B	PDK4	GBA2
CREB1	BDNF	HK1	TMPO	YWHAQ	IGFBP7	CLDN5	COL9A1	MANBA	LPL	AADAC	GGT7
CRTC1	ATO7	LMNA	HTT	DLGAP1	ADIPOR1	SNRNP200	TOB1	CCS	ODC1	ADH7	SLC3A2
PROK2	APOA1	PRKD1	HNRNPK	HNRNPH1	ADIPOR2	LDHD	DSCAM	AK5	PIK3CG	DDAH1	ST3GAL4
PPP1CA	VCP	PGK1	PRDX2	NASP	JUND	NCKAP1	NTM	SLC25A17	SSBP1	MAOB	BAZ1A
PPP1CB	FASN	ACACA	PSMC2	ETV6	PSME1	NCOA4	OPHN1	BRMS1	INTS2	DIO1	CDC16
PPP1CC	YWHAE	MDH2	ATF1	STAT3	PIGF	HLA-DQB1	RGS6	DNAJC2	GBA	EXOSC2	DDHD2
NPY	PAICS	ENO1	VRK3	HTR2C	CYP19A1	RBPMS	RND3	PTGR2	OPRM1	EXOSC3	HMG2
NRIP1	SIN3A	HADHA	HBA2	CGA	CAT	ZFR	DOCK4	ERI1	MC4R	FBP2	CTPS2
RORC	GFPT1	HSP90B1	SRC	GAST	PDE4D	DAZAP2	SEC23IP	NUDT3	HPGDS	IFNB1	MTMR6
SERPINE1	GNB3	NME2	PRDX1	UCP3	EYA1	STBD1	ANKS1B	PPM1L	BAD	VAMP2	RNF40
THRAP3	DRD4	PCCA	RANBP2	ATPIA1	OPCML	GTD1C	IRX1	COQ10B	SCN1A	OSBP	HNRNPA0
MTNR1A	APOB	PCCB	RPL10	NPM1	MYRIP	APOH	LRRC4C	YIF1A	NR5A2	AOC1	MMS19
EZH2	MATR3	VDAC1	RUVBL1	ATPIA3	CUL3	GRM1	RNF19A	SPTSSB	KIF11	EXOSC5	MT1A
RBM4	YTHDF2	CYB5R3	RUVBL2	CRKL	SERPINA7	MMADHC	SORCS1	HIKESHI	PDE4A	TNRC6A	ABHD14B
KDM2A	ADORA1	SLC10A2	RPS14	MCM4	GNA11	HNRNPA2B1	ATP10B	MMP9	TRPV6	GJA1	ATP6V0B
KMT2A	GPR50	HSD17B10	RPS17	TUFM	FBXL17	ST3GAL1	CD180	NRARP	TRPV5	MCL1	GLYATL1
USP2	EXOC1	NME1	PSMC1	YWHAH	SKP2	ING3	FOXN3	ZNF423	GRIK2	BRD4	AGMO
KDM5A	YWHAZ	PRKD3	WDR77	EEF1A2	TGFB2	ITPK1	NAALADL2	MEIS1	MMP2	FXN	ATP5F1D
NONO	CALB1	MCCC2	RAN	EIF4A1	ANP32A	CYP2A6	ARL4A	SCYL1	AKT1	RPA1	WAPL

NAMPT	TXN	MCCC1	NOS2	MCM5	PROKR2	HCRTR1	NCOA7	TAC3	TET2	FDX1	ATP5MC3
RORB	PLAT	CAPZB	CRHR1	C1QBP	PSMA4	MTHFR	NXPH1	SELE	UCP1	RBP1	CIAO2B
CREM	MEF2C	ERO1A	CCNA2	EIF4A2	G0S2	CREB3	RASSF8	PLK4	CREB3L1	TBXT	S100G
NMU	ADCY10	RPE65	TFEB	MCM7	NFKB1	P2RX7	SPCS3	RRBP1	CYP8B1	ABCC1	MSH6
ADCYAP1	HERC2	NGF	KRAS	XRCC6	SDC3	PARP1	TANC2	RND1	RPS6KA5	HMOX2	BACE1
MTNR1B	CHEK1	PIK3R1	FBXO5	KRT10	RPS6KB1	HSD11B2	LCORL	NOTCH1	GCKR	RNF2	SMN2
AHR	SUMO1	THBD	CYP21A2	NXN	EIF4EBP1	STAG2	POF1B	DHFR	CYP1A2	SETD7	S100A1
PRL	EDN1	FAM50B	CAD	PPP2R2A	SCT	PEPC	TXNDC2	HIF1AN	SULT1A3	SREBF2	PTMA
CUL1	EIF2AK3	CDKN3	COPS8	RPN1	PTEN	INSL6	VTA1	MT3	RBL1	RPL4	SPARC
NCOR1	CAMK2G	AGT	DYNC1H1	SLC25A5	SMAD3	SOX14	BRMS1L	USP46	TIMP1	SLC27A1	UBE2N
METTL3	RPSA	TKT	TRPV1	TCP1	SNAI1	FBXL12	KCTD8	HCFC1	PTGS2	CXXC1	ASCL1
MAPK8	EEF2	NOS3	HDAC2	XRCC5	CD63	FBXL6	RHBDD1	RING1	PVALB	PSMD8	RAD18
SFPQ	CPNE8	HSPD1	SLC25A10	XRN2	GPD1	FBXL8	PEL12	SEC13	CDH1	COX11	TOPBP1
KAT2B	FLNA	HNRNP1	TOP2A	DDX20	TXNIP	FBXL22	ZNF662	DMAP1	CCKBR	H2AC6	RAD9A
MAGEL2	MCM3	GRIN2B	FBXO9	EFTUD2	KCNH4	ENSG00000265690	FERD3L	PSMD13	CYP11A1	CASP8	INTS7
SPSB4	CCT2	RPS3	FBXO22	KHDRBS1	BACH1	HSD11B1	MAP9	COX7B	HSPG2	EEA1	RAD1
ID3	CCT8	SOD1	ELANE	KRT2	LY96	ELF5	OR10R2	NUP88	ME1	NFE2L1	NABP2
MTA1	HNRNPA3	UBA1	FGF8	PABPC1	CLEC1B	IL1RN	HDX	RPS4X	RPL38	SLC22A1	ACKR1
PRKCG	HNRNP2	CAND1	PHGDH	PCBP1	HK2	ADRA2A	CTXN3	MED30	PTS	GDF15	PTPRD
IMPDH2	CKAP4	GABBR1	ABCC2	PRDX4	TPT1	ALPP	CDC14C	MED10	IL1A	ATF7	CDC34
UBE3A	IGFBP1	PTPA	SDHA	PTBP1	PLIN1	TGFB1	ZBTB20	CCND1	EIF4G1	BATF3	CLDN1
CDK5	CSNK1G2	SERPINA6	ACLY	USP11	GRIN2C	TAT	BRF1	PRKACB	EIF3B	COP1	CSF1
HIF1A	UBA52	GNAS	MTHFD1	AKAP8	ACHE	AVPR1B	SCP2	PRKACG	TCF7L2	ANGPTL8	NEUROG1
PHLPP1	HNRNPA1	KDM2B	NDUF53	CCT4	TSP0	CP	TSHB	PRKAR1B	BMP4	DLK1	HDAC9
NR0B2	G6PD	GAPDH	GMPS	GPRASP1	PDPK1	HNRNPDL	TCN1	PRODH	BRCA2	CALR	PLP1
ID1	PPP2R1A	CIRBP	EEF1A1	KPNA1	PHB2	ROCK1	TCAP	PRKAR2B	ABCC4	CSN2	PDE12
HCRT	CCK	ALAS1	ALDH9A1	MAP4	HFE	TWIST1	BSX	ADRB3	ALDH2	CDH13	GRIN2A
VIP	SENP1	TFRC	KHSRP	PABPC4	ETS1	ARHGDI3	JUN	DHCR7	LIPE	ADCY5	FN1
SKP1	PPARD	TIMP3	SMC4	CCT6A	RHO	NR1H4	GLUD1	SMC1A	GHSR	GLP1R	GRIN1
HNF4A	TRIM28	NOX4	ANAPC7	DDX17	CYP3A5	TLK2	TDO2	TAF1	DRD1	UBE2I	IRS1
INS	CTNNA1	COMT	HSPA1B	HNRNPF	RBCK1	KISS1	PSEN2	GNS	GNRHR	KMO	ADARB1
LEP	PIWIL1	BVES	BAG2	HNRNPM	ADH4	HSP90AB1	RBX1	NFKB1A	MRGPRX1	PNMT	MAP2K5
CA6	NPY5R	CSE1L	SMC2	ILF3	SF3A3	TPTEP2-CSNK1E	GSK3A	CAMK2D	SCN5A	BAG1	NEFH
DDB1	EGR3	CHEK2	SRM	DDX3Y	LDHA	ENHO	OPRL1	KMT2C	SLC6A2	G6PC2	AKAP13
KLF10	CACUL1	PPP2R5E	DNAJC7	DHX15	TUBB3	ACTL6A	PNOC	SMARCD1	DDB2	ACER2	RAD17
KAT5	FBXL15	ACTN1	ATP5F1A	SCYL2	GSTM3	CTCF	NR4A1	ACBD3	CSNK1G3	HEBP2	SIRPA
RBM4B	RPS6	KRT17	MARS1	GARS1	LDHB	ZNF704	ID4	RFX4	POU1F1	SLC48A1	CD47
USP9X	CD36	GFPT2	DARS1	GEMIN5	IDI1	IL2RA	CYP2C19	PPP4C	TRIM24	RHNO1	CUL4B
PIWIL2	PSMD2	DDX3X	DCTPP1	PABPC3	LDHC	TNRC6B	YY1	SETD2	FOSL2	BOK	GNAZ
SIRT6	CPT1A	CCT5	EPRS1	SEC16A	UGP2	GCH1	KCNH7	HNMT	RBM3	RAB27A	VAMP7
KLF15	UBC	PKM	IARS1	PPP2R2D	VAPA	TYMS	FKBP5	MFSD2A	USP21	PAX6	NES
IL6	NTS	GSN	RARS1	OBI1	AZIN1	TPH2	GFAP	IDH1	NQO2	MGMT	UBE2K
TNF	PSMC3	ACTN4	GCN1	CACNA1C	HLA-DMA	OXT	AHCY	ATF5	PAH	ACTB	AMBRA1
MAPK10	PSMC5	MYH14	CYP7A1	GC	HERPUD1	ATF6	HCN2	IL2	MAT1A	ECE1	DCAF8
MAPK9	PSMD3	DDOST	ERC2	PTGDS	PPP1R3C	DIO2	BLZF1	APOA4	MAT2A	STXBP1	WDR61
SIK1	PSMD11	FLNC	DEFB1	SYVN1	IFNG	PDC	SLC24A3	RARG	QDPR	CPS1	CEBPZ
VIPR2	PSMC6	EZR	CEBPB	RRH	DUSP1	VWF	PLAU	THRA	MECP2	CYP2C8	DCAF7
HUWE1	PSMD1	KRT6A	CYP2D6	SCN8A	OXTR	ADCYAP1R1	MEN1	MYO1D	ST3GAL3	GALNS	INTS3
ASS1	PSEN1	PLEC	CHKA	LMAN1	TRRAP	PFAS	DROSHA	G6PC1	RAPGEF3	MAP2K3	NOL7
DDA1	DCAF11	DET1	PTPDC1	H2BC12L	MIR6883	BTBD9	CARTPT	CDK4	CHRM1	CHRN2	CLDN4
CRX	DDX5	DHX9	DYRK1A	FAS	GHRH	HNF1B	HOMER1	KCND2	KCNMA1	LGR4	MIR1281
MIR3064	MIR4751	MIR5047	MIR5572	MTTP	NLGN1	NPS	NTRK1	NTRK3	OPN3	PAX4	PRF1
PRKAA1	PRKG2	PROK1	ROCK2	SETX	SFTPC	SIX3	UTS2	UTS2R	ZFH3	ELOVL3	DELEC1
CSF2	GHRHR	FBXL21P	TIMELESS	HNRNP2	MYBBP1A	KCNA2					